

# An Efficient Algorithm for Calculating Multiparticle Thermal Interaction in a Concentrated Dispersion of Spheres

ALEXANDER Z. ZINCHENKO\*

*Institute of Mechanics, Moscow University, 119899 Moscow, Russia*

Received March 2, 1992; revised December 7, 1992

The boundary-value problem of heat conduction through a multiparticle system in a medium of a different conductivity  $\lambda_e$  is considered. The particle set is a random arrangement of  $N$  equisized spheres of conductivity  $\lambda'$  in a cubic cell continued periodically into all space. The mean temperature gradient is given. The problem is reduced to an infinite set of equations for the coefficients of the temperature expansion into spherical harmonics on the interfaces. The algorithm exploits the idea that only the interaction of the low-frequency harmonics is long-ranged to construct the "economical truncation," as well as the rotational transformations of spherical harmonics to promote the efficient iterative solution. The method is capable of providing high resolution for arbitrary conductivity ratio  $\gamma = \lambda'/\lambda_e$  and enabling large scale simulations of the effective conductivity of highly concentrated dispersions with various microstructures even on a small computer.

© 1994 Academic Press, Inc.

## 1. INTRODUCTION

Determining the effective properties (heat conductivity, dielectric constant, magnetic permeability, etc.) of a concentrated random dispersion of spheres is a well-known problem of classical physics because of its numerous applications to suspensions, granular materials, and composites. In addition to a great deal of approximate theories the methods for "exact" numerical simulation (i.e., the solution of the boundary-value problem for  $N$  spheres, including averaging over many configurations and the limit  $N \rightarrow \infty$ ) have been developed recently. The method [1] reduces the " $N$ -body problem" to an infinite set of equations for multipole expansion coefficients. The solution of the truncated system is further expanded into powers of  $(\gamma - 1)/(\gamma + 1)$ , producing (via Padé-approximants) upper and lower bounds for the effective conductivity. The strength of this approach, which is quite successful for moderate values of  $\gamma$ , is the analytical dependence of the results upon  $\gamma$  for a given configuration. At the same time, for  $\gamma \gg 1$  and high values of the particle volume fraction  $c$ , the bounds are wide

and strongly affected by the small values of  $N$  (16) and the highest multipole order ( $\leq 7$ ) retained. The newly developed method [2–3] reduces estimation of the conductivity to random walking simulation. This approach (as well as the strategy of parallel iterative solution of boundary integral equations (BIE) on multiprocessor machines proposed in the hydrodynamic aspect [4]) is promising for large systems of arbitrary-shaped inclusions, albeit in the practically interesting case  $1 \ll \gamma < \infty$ , it may require a considerable amount of a supercomputer run time. Finally, the "stokesian dynamics"—like approach [5–6] turns out to be successful for moderately concentrated dispersions with arbitrary  $\gamma$ , as well as for dispersions of superconducting spheres ( $\gamma = \infty$ ) at close packing with exact two-body interactions included in the approximate construction of the capacitance matrix. Unfortunately, for high concentrations and  $1 \ll \gamma < \infty$  the method is sensitive to whether exact two-body interactions are included or not [5–6], and the appropriate choice between the two approximations is not obvious unless the exact solution is obtained.

The published calculations of the effective conductivity of concentrated dispersions of spheres are much less complete than for the two-dimensional problem [2, 7–10]). Besides, successful simulations are still lacking for effective conductivity in random closely packed arrays of highly conducting spheres ( $1 \ll \gamma < \infty$ )—the case of practical significance [11], when the classical Clausius–Mossotti approximation fails completely and the existing exact simulation methods are expected to run into difficulties. So it is of interest to work out a more powerful algorithm for multiparticle interaction of spheres which would be able, in particular, to predict the effective conductivity of granular media. The present method (converging to the exact solution) develops, in particular, the idea of "economical truncation" which proved to be very efficient for two dimensions [9–10]. We start from BIE and reduce the problem to an infinite set of equations, expanding the temperature on the inclusion boundaries into spherical harmonics. The formalism at this stage (Section 2.2 and Appendix A) differs from [1] (being closer to

\* Present address: Department of Chemical Engineering, University of Colorado, Boulder, CO 80309-0424.

that of [12]) and yields the infinite system in the explicit form, avoiding cumbersome calculations. The truncated system matrix is partitioned into near- and far-field parts (not to be confused with the terms "near(far)-field" in [5-6]). The near-field operator is first optimized using the rotational transformations of spherical harmonics by Wigner functions (Section 2.3). Although these functions are familiar in quantum mechanics [13] their application to disperse medium problems seems to be quite new. Then, by the analysis of the Fourier coefficient decrease (Section 2.5), the two operators are economically represented by the sparse matrices (Sections 2.6-2.7) not violating significantly the magnitude of the residual due to the initial truncation. The far-field operator requires calculating lattice sums of arbitrary order and the relevant efficient Ewald-like expressions are proposed in Section 2.8. The "economically truncated" system is solved iteratively by the conjugate gradient method (CGM). The length of the code is quite balanced by its high efficiency which is demonstrated in Section 3, including the comparison with some other methods. The basic ideas of the present algorithm are also applicable to a number of other multiparticle problems which are discussed in Section 4.

All the calculations have been performed on PC AT ACRO 386 C, with Weitek 3167 as a floating point accelerator and about 3 Mbytes of useful memory.

## 2. METHOD

### 2.1. Formulation of the Problem

Consider an infinite set of equisized non-overlapping spheres of radius  $a$ , heat conductivity  $\lambda'$  submerged in a medium of conductivity  $\lambda_e$ . The particle system is obtained from the basic random configuration of spheres  $S_1, \dots, S_N$  centered at  $\mathbf{x}^1, \mathbf{x}^2, \dots, \mathbf{x}^N \in V$  by the triply periodic continuation into all space with the periods 1, 1, 1 ( $V = [0, 1] \times [0, 1] \times [0, 1]$  being the unit cubic cell). The boundary-value problem for the temperature distribution  $T(\mathbf{x})$  has the form

$$\operatorname{div}(\lambda \nabla T) = 0, \quad (1a)$$

$$[T] = \left[ \lambda \frac{\partial T}{\partial n} \right] = 0 \quad \text{for } \mathbf{x} \in S_x \quad (\text{mod}(1, 1, 1)), \quad (1b)$$

$$T(\mathbf{x}) = \mathbf{K} \cdot \mathbf{x} + T_1(\mathbf{x}), \quad (1c)$$

where  $\lambda = \lambda'$  or  $\lambda_e$ ,  $[ ]$  is the jump across the interface,  $\mathbf{n}$  is the outward normal to  $S_x$ . The given vector  $\mathbf{K}$  specifies the mean (over  $V$ ) temperature gradient  $\langle \nabla T \rangle_V = \mathbf{K}$ , and the unknown function  $T_1(\mathbf{x})$  is triply periodic. The problem (1) is uniquely solvable, to within an additive constant in  $T_1$ . It is our main interest to calculate the mean heat flux

$$\langle \mathbf{q} \rangle_V = \langle -\lambda \nabla T \rangle_V = -\lambda_e \mathbf{F} \cdot \mathbf{K} \quad (2)$$

and the corresponding dimensionless effective conductivity tensor  $\mathbf{F}$  (with subsequent averaging over configurations).

### 2.2. Reduction of the Problem to an Infinite Set of Equations

Let  $G(\mathbf{x})$  be the auxiliary triply periodic Green function satisfying

$$\nabla^2 G(\mathbf{x}) = -4\pi + 4\pi \sum_{\mathbf{k}} \delta(\mathbf{x} - \mathbf{k}), \quad \mathbf{k} = (k_1, k_2, k_3), \quad (3)$$

where  $\delta(\mathbf{x})$  is the  $\delta$ -function and the symbol  $\sum$  denotes the summation over all integers  $k_1, k_2, k_3$ . The properties of  $G(\mathbf{x})$ , the well-known function in charged particle physics, are given in [14-15]. Using  $G(\mathbf{x})$  we can first reduce the problem (1) to a system of BIE on  $S_x$  eliminating the artificial boundaries between the cells (unlike the BIE approach [8]). For  $\mathbf{x}$  lying *inside* the continuous phase the Green theorem and (1), (3) yield

$$T_1^e(\mathbf{x}) = C_1 + \frac{1}{4\pi} \sum_{\beta=1}^N \int_{S_\beta} \left[ G(\mathbf{y} - \mathbf{x}) \frac{\partial T_1^e}{\partial n_y} - T_1(\mathbf{y}) \frac{\partial G(\mathbf{y} - \mathbf{x})}{\partial n_y} \right] dS_y, \quad (4)$$

$$C_2 = \frac{1}{4\pi} \sum_{\beta=1}^N \int_{S_\beta} \left[ G(\mathbf{y} - \mathbf{x}) \frac{\partial T_1^e}{\partial n_y} - T_1(\mathbf{y}) \frac{\partial G(\mathbf{y} - \mathbf{x})}{\partial n_y} \right] dS_y.$$

The indices  $e$  and prime mark the values related to the continuous and disperse phases, respectively. The configurationally dependent constants  $C_1, C_2$  are insignificant. Using (1b)-(1c) one can eliminate  $\partial T_1 / \partial n$  from (4). Taking also into account that in the limit  $\mathbf{x} \rightarrow S_x$  the integral over  $S_x$  with the kernel  $\partial G / \partial n_y$  behaves like the usual double-layer potential, we arrive at the system of BIE for the temperature distribution on  $S_x$ ,

$$T^*(\mathbf{x}) = C + \frac{2\mathbf{K} \cdot (\mathbf{x} - \mathbf{x}^z)}{1 + \gamma} + \frac{\kappa}{2\pi} \sum_{\beta=1}^N \int_{S_\beta} T^*(\mathbf{y}) \times \frac{\partial G(\mathbf{y} - \mathbf{x})}{\partial n_y} dS_y, \quad (5)$$

$$\mathbf{x} \in S_x, \quad T^*(\mathbf{x})|_{S_x} = T(\mathbf{x}) - \mathbf{K} \cdot \mathbf{x}^z, \quad \kappa = \frac{\gamma - 1}{\gamma + 1}.$$

The constant  $C$  can be made equal to zero by a suitable shift of  $T_1$ . For the system (5) the values  $\kappa \in [-1, 1)$  are regular. The mean heat flux  $\langle \mathbf{q} \rangle_V$  is expressed in the standard way [16] via particle dipoles:

$$\langle \mathbf{q} \rangle_V = -\lambda_e \mathbf{K} - (\lambda' - \lambda_e) \sum_{x=1}^N \int_{S_x} T^* \mathbf{n} dS. \quad (6)$$

As the next step, we associate with each sphere  $S_\alpha$  the local spherical coordinate system  $(r, \theta, \varphi)$  so that

$$\begin{aligned} (\mathbf{x} - \mathbf{x}^\alpha)_1 &= r \sin \theta \cos \varphi, & (\mathbf{x} - \mathbf{x}^\alpha)_2 &= r \sin \theta \sin \varphi, \\ (\mathbf{x} - \mathbf{x}^\alpha)_3 &= r \cos \theta \end{aligned} \quad (7)$$

(here and henceforth the lower indices of vectors denote their Cartesian components) and a set of Fourier coefficients (FC)  $Z_{nm}^z$ :

$$T^*(\mathbf{x})|_{S_\alpha} = \text{const}_\alpha + \frac{a}{1+\gamma} \sum_{n=1}^{\infty} \sum_{m=-n}^n Z_{nm}^z Y_{nm}(\mathbf{x} - \mathbf{x}^\alpha). \quad (8)$$

For a vector  $\mathbf{r}(r, \theta, \varphi)$  the normalized spherical harmonics are defined as [17]

$$Y_{nm}(\mathbf{r}) = \left[ \frac{(2n+1)(n-m)!}{4\pi(n+m)!} \right]^{1/2} P_n^m(\cos \theta) \exp(im\varphi) \quad (m \geq 0), \quad (9)$$

$$Y_{nm}(\mathbf{r}) = (-1)^m \bar{Y}_{n,-m}(\mathbf{r}) \quad (m \leq 0)$$

with  $P_n^m$  being the associated Legendre function (in the notation of [17–18]) and the overbar denoting complex conjugation.

Substituting (8) into (5) and using the properties of  $G(\mathbf{x})$ , as well as the generalized addition theorem for spherical harmonics, one can obtain an infinite system of equations for the unknowns  $Z_{nm}^z$  (see Appendix A). The system can be symmetrized (and in different ways) which enables the efficient use of conjugate gradient iterations. The simplest form is achieved by introducing the new unknowns

$$U_{nm}^\alpha = \frac{n}{[\pi(2n+1)]^{1/2}} Z_{nm}^\alpha \quad (10)$$

and the infinite set of equations for  $U_{nm}^\alpha$  takes the form

$$\begin{aligned} \frac{2n+1-\kappa}{2n} U_{nm}^\alpha - \frac{4}{3} \pi \delta_{n1} \alpha^3 \kappa \sum_{\beta=1}^N U_{1m}^\beta \\ + \sum_{\beta=1}^N \sum_{v=1}^{\infty} \sum_{\mu=-v}^v \frac{\kappa}{2} (-1)^{v+m} C_{nm} C_{n+v, n-v} C_{v\mu} \\ \times S_{\alpha\beta, v+n}^{\mu-m} U_{v\mu}^\beta = \delta_{n1} f_m, \end{aligned} \quad (11)$$

where

$$\begin{aligned} U_{n,-m}^\alpha &= (-1)^m \bar{U}_{n,m}^\alpha \quad \text{for } m < 0, \\ f_0 &= 2K_3, \quad f_1 = -\bar{f}_{-1} = \sqrt{2} (K_1 - iK_2), \\ C_{nm} &= \frac{1}{2^n} \left[ \frac{(2n)!}{(n-m)! (n+m)!} \right]^{1/2}. \end{aligned} \quad (12)$$

The absolutely convergent lattice sums  $S_{\alpha\beta, v}^\mu$  for  $\alpha \neq \beta$  are introduced as

$$S_{\alpha\beta, v}^\mu = \frac{1}{C_{v\mu}} \left( \frac{4\pi}{2v+1} \right)^{1/2} \sum_{\mathbf{k}} \left( \frac{2a}{|\mathbf{x}^\beta + \mathbf{k} - \mathbf{x}^\alpha|} \right)^{v+1} \times Y_{v\mu}(\mathbf{x}^\beta + \mathbf{k} - \mathbf{x}^\alpha) \quad \text{for } v \geq 3, \quad (13a)$$

$$\begin{aligned} S_{\alpha\beta, 2}^\mu &= \frac{1}{C_{2,\mu}} \left( \frac{4\pi}{5} \right)^{1/2} \left\{ \left( \frac{2a}{|\mathbf{x}^\beta - \mathbf{x}^\alpha|} \right)^3 Y_{2,\mu}(\mathbf{x}^\beta - \mathbf{x}^\alpha) \right. \\ &+ \sum_{\mathbf{k}}' \left[ \left( \frac{2a}{|\mathbf{x}^\beta + \mathbf{k} - \mathbf{x}^\alpha|} \right)^3 Y_{2,\mu}(\mathbf{x}^\beta + \mathbf{k} - \mathbf{x}^\alpha) \right. \\ &\left. \left. - \left( \frac{2a}{|\mathbf{k}|} \right)^3 Y_{2,\mu}(\mathbf{k}) \right] \right\}. \end{aligned} \quad (13b)$$

For  $\alpha = \beta$  and  $v \geq 3$  the definition (13a) also holds, with  $\sum$  replaced by  $\sum'$ . Finally,  $S_{\alpha\alpha, 2}^\mu = 0$ . The classical sums  $S_{\alpha\alpha, v}^\mu$  are all real.

The mean heat flux (6) is

$$\langle q_1 + iq_2 \rangle_v = -\lambda_e \left[ K_1 + iK_2 + 2\pi \sqrt{2} \kappa a^3 \sum_{z=1}^N \bar{U}_{1,1}^z \right], \quad (14)$$

$$\langle q_3 \rangle_v = -\lambda_e \left[ K_3 + 2\pi \kappa a^3 \sum_{z=1}^N U_{1,0}^z \right].$$

It can be seen from (11), (14) that the deviation of the conductivity tensor  $\mathbf{F}$  from the Maxwell–Clausius–Mossotti formula,

$$\mathbf{F} = \frac{\gamma + 2 + 2(\gamma - 1)c}{\gamma + 2 - (\gamma - 1)c} \mathbf{I}, \quad (15)$$

is solely due to the non-zero coefficients  $S_{\alpha\beta, v+n}^{\mu-m}$  in (11).

For non-touching spheres the system (11) (unlike (5)) has  $\kappa = 1$  as a regular value (the simple proof [9] also holds for three dimensions), which enables the limit of superconducting spheres. Furthermore, (11) is a self-adjoint positive definite system. Indeed, this is true for  $\kappa = 0$ . Since all the eigenvalues are real and non-zero for  $\kappa \in [-1, 1]$ , they remain positive.

The traditional numerical approach to (11) would be the truncation

$$U_{nm}^\alpha = 0 \quad \text{for } n > k_0 \quad (16)$$

(“ $k_0$ -family of approximations”), with the convergence to the exact solution at  $k_0 \rightarrow \infty$ . Obviously, direct solutions of (11), (16) are impracticable for any large values of  $N$  and  $k_0$ . The very suitable iterative scheme is CGM, especially for high  $c$  and  $\gamma \gg 1$ , since it is weakly sensitive to small gaps between the particles (see Section 3). However, for  $N, k_0 \gg 1$

the cost of each iteration remains still very prohibitive. Assuming that all  $\approx (Nk_0)^2$  independent coefficients  $S_{\alpha\beta, \nu}^\mu$  are calculated in advance (which is a problem itself), each iteration requires approximately

$$k_0^2(k_0 + 3)^2 N(N - \frac{1}{2}) \quad (17)$$

floating point (FP) multiplications and a close number of additions (for the optimized code) and would take about 1.2 h for  $N=100$ ,  $k_0=20$  on a 1 Mflop/s performance machine.

The main purpose of the present paper is to demonstrate that the amount (17) for  $N, k_0 \gg 1$  can be very significantly reduced (even by two orders of magnitude in practice), in part by some modification of the truncated system (11), (16), whereas the error remains essentially the same.

Let  $\mathbf{k}_{\alpha\beta}$  ( $\alpha \neq \beta$ ) be the integer vector so that  $\mathbf{x}^\beta + \mathbf{k}_{\alpha\beta}$  is the center of the periodically replicated  $S_\beta$  that is nearest to  $S_\alpha$  and

$$\mathbf{R}_{\alpha\beta} = \mathbf{x}^\beta + \mathbf{k}_{\alpha\beta} - \mathbf{x}^\alpha, \quad \zeta_{\alpha\beta} = |\mathbf{R}_{\alpha\beta}|/a. \quad (18)$$

The starting point of our method is to single out the contribution of this nearest image from the lattice sums:

$$S_{\alpha\beta, \nu}^\mu = \frac{1}{C_{\nu\mu}} \left( \frac{4\pi}{2\nu + 1} \right)^{1/2} \left( \frac{2}{\zeta_{\alpha\beta}} \right)^{\nu+1} Y_{\nu\mu}(\mathbf{R}_{\alpha\beta}) + (S')_{\alpha\beta, \nu}^\mu. \quad (19)$$

Extending the definition  $(S')_{\alpha\beta, \nu}^\mu = S_{\alpha\beta, \nu}^\mu$ , we can split the triple truncated sum (11) into two operators:

The near-field operator  $\mathcal{A}^*$ :

$$\begin{aligned} (\mathcal{A}^*U)_{nm}^\alpha &= \frac{\kappa}{2} C_{nm} \sum_{\substack{\beta=1 \\ \beta \neq \alpha}}^N \sum_{v=1}^{k_0} (-1)^{\nu+m} \left( \frac{4\pi}{2\nu + 2n + 1} \right)^{1/2} \\ &\times \left( \frac{2}{\zeta_{\alpha\beta}} \right)^{n+\nu+1} C_{n+\nu, n-\nu} \sum_{\mu=-\nu}^{\nu} \frac{C_{\nu\mu}}{C_{n+\nu, \mu-m}} \\ &\times Y_{\nu+n, \mu-m}(\mathbf{R}_{\alpha\beta}) U_{\nu\mu}^\beta \end{aligned} \quad (20)$$

and the far-field operator  $\mathcal{A}^{**}$

$$\begin{aligned} (\mathcal{A}^{**}U)_{nm}^\alpha &= \frac{\kappa}{2} C_{nm} \sum_{\beta=1}^N \sum_{v=1}^{k_0} (-1)^{\nu+m} C_{n+\nu, n-\nu} \\ &\times \sum_{\mu=-\nu}^{\nu} (S')_{\alpha\beta, \nu+n}^{\mu-m} C_{\nu\mu} U_{\nu\mu}^\beta. \end{aligned} \quad (21)$$

The two operators are calculated in very different ways.

### 2.3. The $O(N^2 k_0^3)$ -Rotational Algorithm for the Near-Field Operator

It is remarkable that for  $k_0 \gg 1$  the operator  $\mathcal{A}^*$  can be calculated much faster than by the direct summation (20)

and without any new approximations. It follows from (9) that if  $\mathbf{R}_{\alpha\beta}$  were directed along the  $x_3$ -axis there would be splitting with respect to the azimuthal number  $m$ ; i.e., the only term with  $\mu = m$  would contribute to the inner sum (20). To make use of this, we note that, according to our derivation of (11) (see Appendix A), the RHS of (20) for a single  $\beta$  represents the action of the *invariant* operator

$$\frac{\kappa}{2\pi} \int_{S_\beta} T^*(\mathbf{y}) \frac{\partial}{\partial n_y} \left( \frac{1}{|\mathbf{y} + \mathbf{k}_{\alpha\beta} - \mathbf{x}|} \right) dS_y \quad (22)$$

in the coordinate form, yielding (up to the factor  $[4\pi/(2n+1)]^{1/2}$ ) the  $(n, m)$ -Fourier coefficients of the distribution (22) on  $S_\alpha$ , with any  $T^*|_{S_\beta}$  represented by the truncated Fourier series. Hence, the action of (22) can be first calculated in a special coordinate system, with the subsequent transformation to the initial coordinates. That is the idea behind our algorithm.

Let us rotate the initial local coordinate system  $(x_1, x_2, x_3)$  (originated at  $\mathbf{x}_\beta + \mathbf{k}_{\alpha\beta}$ ) to a new position  $(x'_1, x'_2, x'_3)$  superposing the unit vector of the  $x_3$ -axis with  $\mathbf{R}_{\alpha\beta}/R_{\alpha\beta}$ , for a chosen pair  $(\alpha, \beta)$  ( $1 \leq \alpha < \beta \leq N$ ). This rotation is a sequence of two transformations: (1) rotation about the  $x_3$ -axis of angle  $\chi_{\alpha\beta}$ ; (2) rotation about the new  $x_1$ -axis of angle  $\psi_{\alpha\beta}$ , where

$$\begin{aligned} \exp(i\chi_{\alpha\beta}) &= (-X_2 + iX_1)/(X_1^2 + X_2^2)^{1/2}, \\ 0 &\leq \chi_{\alpha\beta} < 2\pi, \\ \eta &= \cos \psi_{\alpha\beta} = X_3/R_{\alpha\beta}, \quad 0 \leq \psi_{\alpha\beta} < \pi, \\ \mathbf{R}_{\alpha\beta} &= (X_1, X_2, X_3) \end{aligned} \quad (23)$$

(in the degenerate case  $X_1 = X_2 = 0$  the value of  $\chi_{\alpha\beta}$  is arbitrary). The third Euler angle in our case can be set to zero. Let  $(r', \theta', \varphi')$  (subsequently referred to as the "axial system for  $\alpha, \beta$ ") be the local spherical coordinates associated with  $x'_1, x'_2, x'_3$ . It follows from the theory of Wigner functions [17] that

$$\begin{aligned} Y_{lm}(\theta, \varphi) &= \sum_{|m'| \leq l} \exp(im\chi_{\alpha\beta}) P_{mm'}^l(\psi_{\alpha\beta}) Y_{lm'}(\theta', \varphi'), \\ Y_{lm'}(\theta', \varphi') &= \sum_{|m| \leq l} (-1)^{m+m'} \exp(-im\chi_{\alpha\beta}) \\ &\times P_{m'm}^l(\psi_{\alpha\beta}) Y_{lm}(\theta, \varphi). \end{aligned} \quad (24)$$

The coefficients  $P_{mm'}^l$  obey

$$P_{mm'}^l = P_{m'm}^l, \quad P_{mm'}^l = P_{-m, -m'}^l \quad (25)$$

and are related to Jacobi polynomials [17]. Of course, it is very prohibitive to calculate in advance and store all the necessary  $P$ -coefficients. Instead, in our algorithm they are

recalculated repeatedly. It is convenient to introduce the new real  $X$ -coefficients,

$$P_{mm'}^l(\psi_{\alpha\beta}) = i^{|m'| - m} (C_{lm'}/C_{lm}) X_{mm'}^l \quad (\text{for } |m'| \leq m \leq l), \quad (26)$$

and the most efficient computational scheme for  $X_{mm'}^l$  turns out to be

$$X_{0,0}^0 = 1, \quad X_{l,\pm l}^l = \frac{\eta \pm 1}{2} X_{l-1,\pm(l-1)}^{l-1} \quad (\text{for } l \geq 1), \quad (27a)$$

$$X_{lm'}^l = \frac{1}{2} \sin \psi_{\alpha\beta} X_{l-1,m'}^{l-1} \quad (\text{for } |m'| \leq l-1), \quad (27b)$$

$$X_{mm'}^l = \frac{1}{l-m} [(l\eta - m') X_{mm'}^{l-1} - l \sin \psi_{\alpha\beta} X_{m+1,m'}^{l-1}] \quad (\text{for } |m'| \leq m \leq l-1) \quad (27c)$$

(for  $m = l-1$  the last term in (27c) is set to zero). Let the coordinate system  $(\theta', \varphi')$  on  $S_x$  be a mere translation of the  $(\theta, \varphi)$ -system from  $\mathbf{x}_\beta + \mathbf{k}_{\alpha\beta}$ . The economical way to calculate the transformation  $(U_{\nu\mu})'$  of the coefficients  $U_{\nu\mu}$  into the  $(\theta', \varphi')$ -system (either on  $S_x$  or  $S_\beta$ ) is to compute first the real arrays  $a_m, b_m, c_m, d_m$  ( $0 \leq m \leq k_0$ ),

$$a_m + ib_m = C_{\nu m} i^m \exp(im\chi_{\alpha\beta}) U_{\nu m} \quad (\text{for } m > 0), \quad (28)$$

$$a_0 = \frac{1}{2} U_{\nu 0} C_{\nu 0},$$

$$c_m + id_m = \frac{1}{C_{\nu m}} i^{-m} \exp(im\chi_{\alpha\beta}) U_{\nu m};$$

then for  $m' \geq 0$ ,

$$C_{\nu m'} (U_{\nu m'})' = i^{-m'} \sum_{m=0}^{m'} [a_m (X_{m'm}^\nu + X_{m',-m}^\nu) + ib_m (X_{m'm}^\nu - X_{m',-m}^\nu)] + (C_{\nu m'})^2 i^{m'} \times \sum_{m=m'+1}^{\nu} [c_m (X_{mm'}^\nu + X_{m,-m'}^\nu) + id_m (X_{mm'}^\nu - X_{m,-m'}^\nu)]. \quad (29)$$

Similar relations for the inverse transformation can be also obtained.

Our algorithm acts in the following way:

1. Initialize  $(\mathcal{A}^*U)$  (dots denote arbitrary admissible indices).

2. For all  $(\alpha, \beta)$ -pairs ( $1 \leq \alpha < \beta \leq N$ ):

2.1. Calculate  $\mathbf{R}_{\alpha\beta}, \cos \psi_{\alpha\beta}, \sin \psi_{\alpha\beta}, \exp(i\chi_{\alpha\beta})$  from (23).

2.2. Calculate the array

$$S_\nu = \frac{\kappa}{2C_{\nu 0}} \left( \frac{2}{\zeta_{\alpha\beta}} \right)^{\nu+1}, \quad 2 \leq \nu \leq 2k_0.$$

2.3. For  $\nu = 1, \dots, k_0$  compute  $X_{\nu\nu}^\nu$ -coefficients via  $X_{\nu\nu}^{\nu-1}$  using (27) and the rotational transformations  $(U_{\nu\nu}^\alpha)'$ ,  $(U_{\nu\nu}^\beta)'$  of  $U_{\nu\nu}^\alpha, U_{\nu\nu}^\beta$  into the  $(\theta', \varphi')$ -system, using (28)–(29).

2.4. For  $n = 1, \dots, k_0$ :

2.4.1. Calculate  $X_{nn}^n$ -coefficients via  $X_{nn}^{n-1}$ .

2.4.2. Compute simultaneously the (simplified) contributions ( $0 \leq m \leq n$ )

$$C_{nm} \sum_{\nu=\max(m,1)}^{k_0} (-1)^{\nu+m} C_{n+\nu, n-\nu} S_{n+\nu} [C_{\nu m} (U_{\nu m}^\beta)'] \quad (30)$$

of  $\beta$ -particle to  $(\mathcal{A}^*U)_{nm}^\alpha$  and

$$C_{nm} (-1)^{n+m} \sum_{\nu=\max(m,1)}^{k_0} C_{n+\nu, n-\nu} S_{n+\nu} [C_{\nu m} (U_{\nu m}^\alpha)'] \quad (31)$$

of  $\alpha$ -particle to  $(\mathcal{A}^*U)_{nm}^\beta$ , both in the new system  $(\theta', \varphi')$ .

2.4.3. Transform (30)–(31) back to the initial system using  $X_{nn}^n$  and add to the current values of  $(\mathcal{A}^*U)_{nn}^\alpha$  and  $(\mathcal{A}^*U)_{nn}^\beta$ .

For each  $(\alpha, \beta)$ -pair the optimized code requires  $2k_0(3k_0^2 + 12k_0 + 11)$  multiplications on the inner loops plus two square roots for step 2.1 (The elimination of step 2.4.1 is unjustified since it would require considerable additional memory, with only a small ( $< 17\%$ ) increase in efficiency). For  $k_0 = 10, 20$  this estimate predicts, respectively, 3.9- and 7.3-fold advantages of the rotational algorithm over the best code for the direct summation (20), compared to 3- and 6-fold acceleration in actual computer tests.

#### 2.4. What is the Economization

It should be emphasized that (16) is only a conventional way to reduce the problem to a finite-dimensional one. For  $N, k_0 \gg 1$  the truncation (16) alone becomes extremely inefficient. Indeed, only a small portion of the interactions between the coefficients  $U_{n\nu}^\alpha$  and  $U_{\nu n}^\alpha$  in (11), namely, with  $n, \nu = O(1)$  are long-ranged. Hence it is attractive to try setting a lot of other interactions in the truncated system (11), (16) to zero so that the error of approximation would remain essentially the same as for the initial truncation (16). On doing this we obtain a new family of “modified  $k_0$ -approximations” converging to the same limit at  $k_0 \rightarrow \infty$ , but the cost of an iterative solution is much reduced since the approximations are now made by *sparse* matrices. This idea of “economization” proved to be very efficient for two dimensions [9–10]. To realize it systematically for spheres,

we also need first the information about the behavior of the FC  $Z_{nm}^\alpha$  (or  $U_{nm}^\alpha$ ) for the *exact* solution at  $n \rightarrow \infty$ . In particular, knowing this we could estimate the residual due to the truncation (16).

### 2.5. Rate of Decrease of Fourier Coefficients

In the two-dimensional problem the following *exact* result [9] was established. For any multiparticle configuration of *equisized* superconducting circles ( $\equiv$  cylinders), with or without periodic replication: (1) The asymptotics of the higher-order FC on  $S_\alpha$  is, up to a factor, the same, as if  $S_\alpha$  were interacting only with its nearest neighbor  $S_\beta$  alone in the unbounded medium, *even if*  $S_\alpha$  is not the nearest neighbor of  $S_\beta$ ; (2) Given more than one particle nearest to  $S_\alpha$  the FC asymptotics for  $S_\alpha$  is a certain linear combination of two-particle asymptotics for its interaction with all the nearest neighbors.

For spheres it is inconvenient to study the behavior of all coefficients  $U_{nm}^\alpha$  because of their dependence on a particular choice of a coordinate system. Instead, we introduce

$$U_n^\alpha = \left[ \sum_{m=-n}^n |U_{nm}^\alpha|^2 \right]^{1/2}, \quad (32)$$

$$Z_n^\alpha = \frac{[\pi(2n+1)]^{1/2}}{n} U_n^\alpha.$$

The rotational transformation of harmonics  $Y_n$  is made by an orthogonal matrix [13, 17], thus implying the invariance of (32). The coefficients  $Z_n^\alpha$  have some physical meaning, being connected with the temperature fluctuation on  $S_\alpha$ :

$$\int_{S_\alpha} (T(\mathbf{x}) - \langle T \rangle_{S_\alpha})^2 d\Omega = \frac{a^2}{(1+\gamma)^2} \sum_{n=1}^{\infty} (Z_n^\alpha)^2. \quad (33)$$

The validity of the result [9] for spheres could be justified, in part, by lengthy arguments similar to those of [9] since the lemma [9] about the structure of the inverse point set also holds for three dimensions. However, for brevity, we shall simply confirm the applicability of the conclusion [9] for spheres of arbitrary conductivity up to touching by a comprehensive numerical analysis.

Consider first a finite cloud of particles  $S_1, \dots, S_N$  in an unbounded medium with the temperature gradient  $\mathbf{K}$  at infinity. The relations (11)–(12), (18)–(19) also hold for this case, with  $\mathbf{k}_{\alpha\beta}$ ,  $(S')_{\alpha\beta, \nu}^\mu$ ,  $S_{\alpha\nu}^\mu$  and the “excluded volume term”  $\frac{4}{3} \delta_{n1} \pi a^3 \kappa \dots$  all set to zero. In particular, for  $N=2$  and  $\mathbf{K}$  being the unit vector parallel ( $m=0$ ) or normal ( $m=1$ ) to the line of centers we have (in the axial system for  $S_1, S_2$ ) the closed relation

$$\frac{2n+1-\kappa}{2n} U_{nm} = \kappa_m \sum_{v=1}^{\infty} \frac{(n+v)! \zeta^{-(n+v+1)} U_{vm}}{[(n-m)! (n+m)! (v-m)! (v+m)!]^{1/2}} + \delta_{n1} 2^{1-m/2} \quad (n \geq 1), \quad (34)$$

$$\zeta = \zeta_{12}, \quad \kappa_m = (-1)^m \kappa, \quad U_{nm} = U_{nm}^1 = (-1)^{n-1} U_{nm}^2.$$

The behavior of  $U_{nm}$  at  $n \rightarrow \infty$  can be found analytically in the spirit of Laplace and the saddle point methods (see Appendix B). These expressions explain clearly why even for almost touching superconductors, as well as for touching spheres of large (but finite) relative conductivity the accurate numerical solution based on spherical harmonics can be quite successful. But, unfortunately, the analytical formulae of Appendix B for non-touching spheres are generally not uniformly valid up to  $\zeta = 2$ , since there is no match with the contact asymptotics (B3). So, the analytical approach provides useful, but, for the present, incomplete information. For this reason in our algorithm the rate of

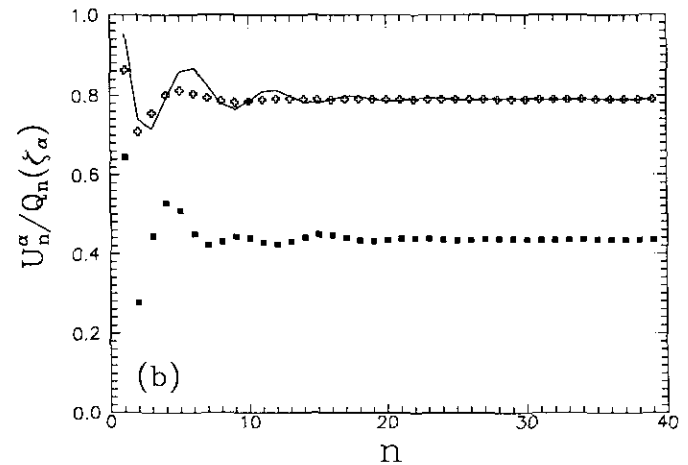
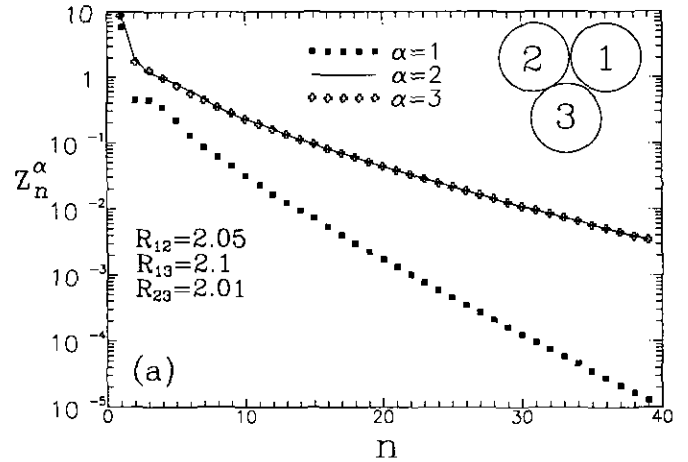


FIG. 1. The Fourier coefficients for three superconducting spheres in the general configuration:  $\mathbf{x}^1 = \mathbf{0}$ ,  $\mathbf{x}^2 = (1.025, 1.221151, -1.288668)$ ,  $\mathbf{x}^3 = (1.743880, 1.017639, 0.577315)$ .

decrease of FC for two spheres is estimated uniformly well by the positive monotonic sequence  $Q_n(\zeta)$ , which is, by definition, the numerical solution of (34) with  $m=0$  for  $\kappa > 0$  and  $m=1$  for  $\kappa < 0$  (thus the second oscillatory solution, which is always much smaller numerically, is omitted).

For a multiparticle system the following estimate is proposed:

$$U_n^\alpha \sim Q_n(\zeta_\alpha), \quad \zeta_\alpha = \min_{\beta: \beta \neq \alpha} \zeta_{\alpha\beta} \quad (35)$$

The validity of (35) was verified for a large number of three-particle configurations with different  $\gamma$ . Some of the results are given in Figs. 1–3, with  $a=1$ ,  $\mathbf{K}=(0, 0, 1)$ . The coefficients  $U_{nm}^x$  were computed from the infinite system truncated by (16) using CGM and our rotational algorithm for  $\mathcal{A}^*$ . To ensure accuracy for higher-order coefficients, large (and different) values of  $k_0$ , up to 100, were used, the error in  $U_n^x$  being within 2% for Fig. 2 and much smaller for Figs. 1, 3. For  $k_0=100$  the coefficients  $U_n^x$  ( $n < 40-50$ )

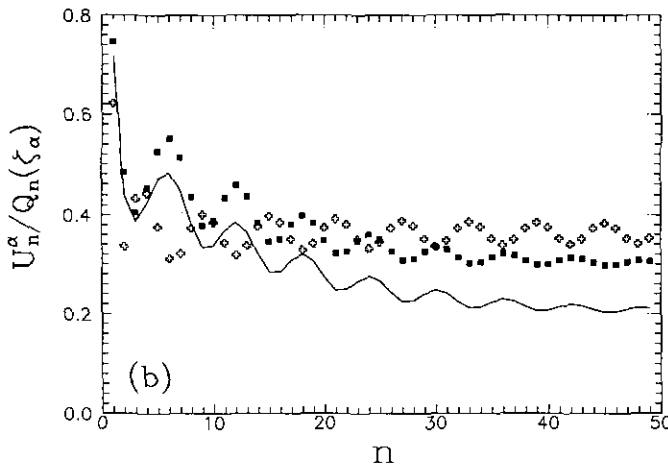
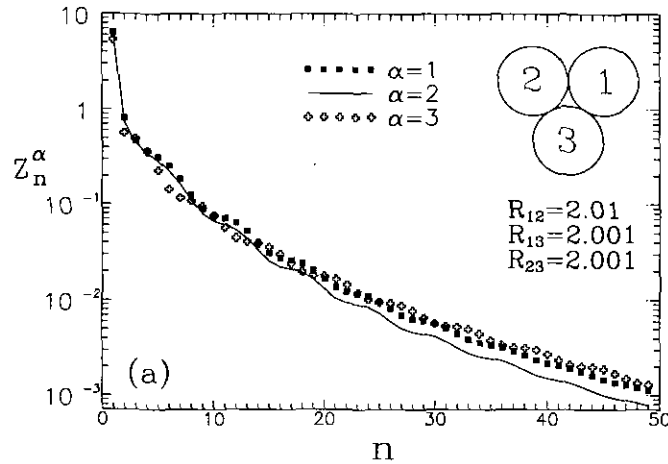


FIG. 2. The Fourier coefficients for three spheres of finite relative conductivity  $\gamma=20$  in the isosceles configuration:  $\mathbf{x}^1=0$ ,  $\mathbf{x}^2=(1.206, -1.071559, 1.198927)$ ,  $\mathbf{x}^3=(-0.608218, -1.765717, 0.718551)$ .

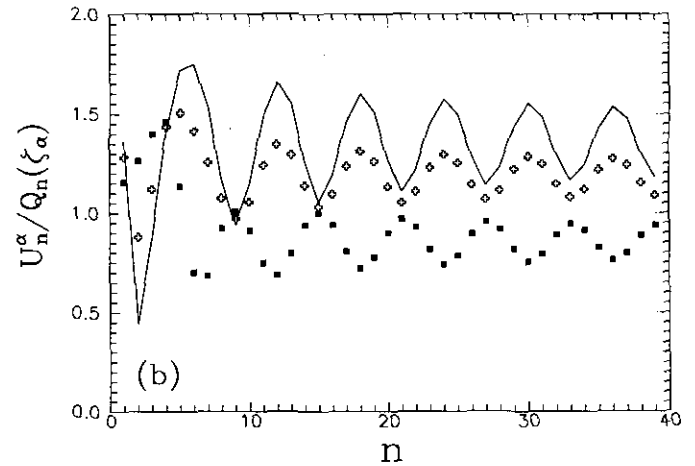
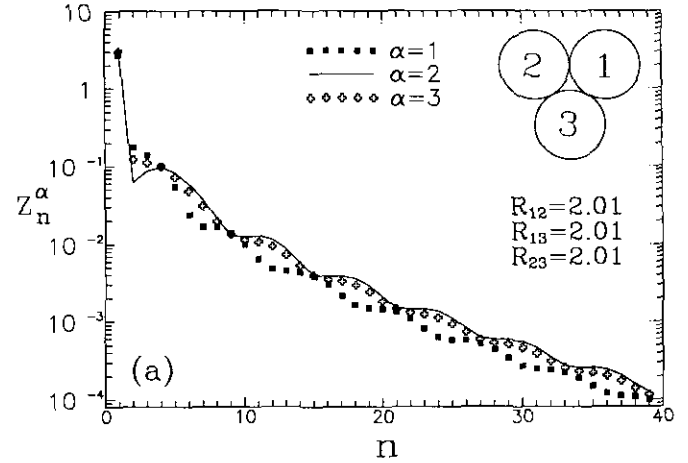


FIG. 3. The Fourier coefficients for three insulating spheres in the equilateral configuration:  $\mathbf{x}^1=0$ ,  $\mathbf{x}^2=(1.206, -0.605223, -1.489755)$ ,  $\mathbf{x}^3=(-0.615498, 0.134171, -1.908733)$ .

normally converged to five figures after about 20 iterations ( $\approx 17$  min of the CPU time).

Figures 1–3 show that the ratio  $U_n^\alpha/Q_n(\zeta_\alpha)$  remains always of the order  $O(1)$  at  $n \rightarrow \infty$ , both for general and for special configurations with more than one nearest neighbor of  $S_\alpha$ . It should be stressed that the validity of (35) is by no means connected with the so-called “pairwise additivity approximation” since the values of  $U_n^\alpha/Q_n(\zeta_\alpha)$  are determined by essentially multiparticle interaction. E.g., for Fig. 1 the exact values 0.44, 0.79, 0.79 of  $U_n^\alpha/Q_n(\zeta_\alpha)$  at large  $n$  would be replaced, in a pairwise additive fashion, by 0.63, 0.93, 0.93, respectively.

For a multiparticle system with periodic replication the estimate (35) also holds, the only difference being in the definition (18) of  $\mathbf{R}_{\alpha\beta}$ . The numerical example demonstrating the validity of (35) for this case is given a posteriori in Section 3.

## 2.6. Near-Field Economization

In the space of infinite sequences  $U_{nm}^z$  ( $|m| \leq n < \infty$ ) with  $U_n^z \rightarrow 0$  ( $n \rightarrow \infty$ ) the following norm is used

$$\|U\| = \frac{1}{N} \sum_{\alpha=1}^N \max_{n: 1 \leq n < \infty} U_n^z. \quad (36)$$

The solution of (11), (16) should be properly understood as the solution of the *infinite* system with the truncated matrix, i.e., with  $\infty$  in (11) replaced by  $k_0$  for  $n \leq k_0$  and by zero for  $n > k_0$ . This implies that the norm  $h$  of the residual arising from substituting the exact solution of (11) into the omitted terms is

$$h = \frac{1}{N} \sum_{\alpha=1}^N \max \left\{ \max_{n: n > k_0} \left[ \frac{(2n+1-\kappa)}{2n} U_n^z \right], \max_{n: 1 \leq n \leq k_0} \phi_n^z \right\}, \quad (37)$$

where  $\phi_{nm}^z$  is the triple sum (11) with the summation limit  $v=1$  replaced by  $v=k_0+1$ . To estimate  $\phi_{nm}^z$  for  $k_0 \gg 1$ , only one value of  $\beta$ , for the nearest image to  $S_\alpha$ , can be retained, with  $S_{\alpha\beta, v}^\mu$  replaced by the first term of (19). Further, the validity of (35) can be explained only by the presence of the corresponding two-particle constituent in the asymptotic expansion of  $U_{\nu\mu}^\beta$  for  $v \gg 1$ , even if  $S_\alpha$  (or any of its images) is not the nearest neighbor of  $S_\beta$ . Substituting this constituent into  $\phi_{nm}^z$  yields the only *non-oscillating* term. Using the axial system for  $\alpha, \beta$ , we can write the estimate for  $\phi_n^z$  in this manner as (see (30)–(31))

$$\phi_n^z \sim C_{nm} \sum_{v=k_0+1}^{\infty} C_{n+v, n-v} |S_{n+v}| C_{vm} Q_v(\zeta_\alpha) \quad (38)$$

with  $m=0$  ( $\kappa > 0$ ) or  $m=1$  ( $\kappa < 0$ ) (judging by the validity of (35), the other values of  $m$  can be neglected for *estimating*  $\phi_n^z$ ). For the first term in the braces (37), the estimate (35) is also used. In both cases we neglect the difference in the numerical factors before  $Q_n(\zeta_\alpha)$  for different  $\alpha$  (considering it to be of minor importance); then, without any loss of generality, the factors are simply set to unity (see Section 3). The numerical calculations of (38) show that the first term in (37) always dominates, and for  $k_0 \gg 1$  we arrive at the quite natural estimate

$$h = \frac{1}{N} \sum_{\alpha=1}^N Q_{k_0+1}(\zeta_\alpha). \quad (39)$$

The next step is to construct the *barrier function*  $v^*(\alpha, \beta, n)$  and restrict the summation over  $v$  in (20) by  $1 \leq v \leq v^*$  so that only a small portion of the coefficients in the near-field matrix is retained and, at the same time, the

residual remains of the order (39). We use a simple inequality

$$\left[ \sum_{m=-n}^n |(\mathcal{A}^* U)_{nm, v}^{\alpha\beta}|^2 \right]^{1/2} \leq \frac{|\kappa| (n+v)!}{v! n! \zeta_{\alpha\beta}^{n+v+1}} U_v^\beta, \quad (40)$$

where  $(\mathcal{A}^* U)_{nm, v}^{\alpha\beta}$  is the RHS of (20) without summation over  $\beta$  and  $v$ . To prove (40), we note that the LHS of (40) is related to the norm (32) of the Fourier coefficients for the distribution (22) on  $S_\alpha$ , with  $T^* |S_\beta$  represented by (8) with  $n=v$ . Hence, the LHS of (40) is rotationally invariant as well as the RHS and it is sufficient to prove (40) in the axial system for  $\alpha, \beta$ , where it becomes evident from

$$\sum_{m: |m| \leq \alpha, v} \frac{|U_{vm}^\beta|^2}{(n-m)! (n+m)! (v-m)! (v+m)!} \leq \left( \frac{1}{n! v!} \right)^2 \sum_{m=-v}^v |U_{vm}^\beta|^2. \quad (41)$$

There may be slightly different procedures of specifying  $v^*$ . The proposed way to “share the residual” among the particles is

$$\sum_{v=v^*(\alpha, \beta, n)+1}^{k_0} \frac{|\kappa| (v+n)!}{v! n! \zeta_{\alpha\beta}^{v+n+1}} Q_v(\zeta_\beta) < \frac{\chi h N}{(\zeta_{\alpha\beta})^4} \left[ 2 \sum_{1 \leq \alpha < \beta \leq N} \zeta_{\alpha\beta}^{-4} \right]^{-1} \quad (42)$$

with  $\chi = O(1)$  being some fixed numerical factor. Here  $v^*$  is the minimum value satisfying (42) and  $\zeta^{-4}$  is chosen as the *simplest function integrable at infinity* in  $\mathbb{R}^3$  to retain the applicability of the method in the limit  $N \rightarrow \infty$ . The *inequality* (40), the definition (42) of  $v^*$ , and Cauchy inequality rigorously imply that the norm (36) of the omitted terms (with  $v > v^*$ ) in (20) is less than  $\chi h$ , provided that the exact solution estimate (35) is used for all  $n$ . Note that both the summation and the factors  $Q_v(\zeta_\beta)$  in the LHS of (42) strongly affect the bounds  $v^*$  for close particles. Judging by the two-dimensional analysis [9] a more obvious criterion for the selection of significant interactions in  $\mathcal{A}^*$  just by the magnitude of the coefficients would be much less efficient.

The use of  $v^*(\alpha, \beta, n)$  in (20) would violate the self-adjointness of  $\mathcal{A}^*$  undesirably, so the next step is to replace  $v^*$  by the rougher *symmetric* function  $k_0^*(\alpha, \beta)$  constructed as follows.

Let  $\zeta_\alpha \geq \zeta_\beta$ , then  $Q_n(\zeta_\beta) \geq Q_n(\zeta_\alpha)$ . Since  $v^*(\alpha, \beta, 1) > 0$  is always met in practice, two possibilities may occur:

1.  $v^*(\alpha, \beta, n) > 0$  for all  $n \leq k_0$ ; then we set  $k_0^*(\alpha, \beta) = k_0$ .



2.  $v^*(\alpha, \beta, n^* + 1)$  becomes zero for some  $n^* \in [1, k_0 - 1]$ ; then  $v^*$  remains zero for  $n > n^* + 1$  (according to all test calculations) and we set

$$k_0^*(\alpha, \beta) = \max \left[ \max_{n: 1 \leq n \leq n^*} v^*(\alpha, \beta, n), n^* \right]. \quad (43)$$

If  $\zeta_\alpha < \zeta_\beta$  we set  $k_0^*(\alpha, \beta) = k_0^*(\beta, \alpha)$ . Once  $k_0^*$  has been specified, the only change in the rotational algorithm of Section 2.3 is to replace  $k_0$  by  $k_0^*(\alpha, \beta)$  for each  $(\alpha, \beta)$ -pair, but for  $N, k_0 \gg 1$  the effect is very pronounced since  $k_0^*(\alpha, \beta)$  is close (or equal) to  $k_0$  only for  $\zeta_{\alpha\beta} \approx 2$ .

The efficiency of this economized algorithm for  $\mathcal{A}^*$  is characterized by

$$c_{nf} = \frac{\sum_{1 \leq \alpha < \beta \leq N} 2k_0^*(\alpha, \beta) [3(k_0^*(\alpha, \beta))^2 + 12k_0^*(\alpha, \beta) + 11]}{k_0^2(k_0 + 3)^2 N(N - 1/2)} \quad (44)$$

which is, approximately, the number of FP multiplications relative to (17).

The elements  $Q_n(\zeta_\alpha)$ ,  $k_0^*(\alpha, \beta)$  are calculated before iterations. For  $Q_n(\zeta_\alpha)$  the CGM is used, with the truncation bound of (34) being several times as large as  $k_0$ . The particles are rearranged so that  $\zeta_1 \geq \zeta_2 \geq \dots \geq \zeta_N$ . In this case  $Q_n(\zeta_\alpha)$  are good initial approximations (if not the exact values) for  $Q_n(\zeta_{\alpha+1})$ . High accuracy is not required for  $Q_n(\zeta_\alpha)$  and this stage takes only a small portion of the total computation time.

### 2.7. Far-Field Economization and the Higher-Order Lattice Sums

For the far-field operator the economization is made somewhat differently. The interaction between  $U_{1m}^\alpha$  and  $U_{1\mu}^\beta$  in (21) is always retained (and, moreover, calculated exactly). According to (13a), (18)–(19), for  $v \geq 3$

$$(S')_{\alpha\beta, v}^\mu = \frac{1}{C_{v\mu}} \left( \frac{4\pi}{2v+1} \right)^{1/2} \sum_{\mathbf{k}} \left( \frac{2}{\zeta_{\alpha\beta, \mathbf{k}}} \right)^{v+1} Y_{v\mu}(\mathbf{R}_{\alpha\beta} + \mathbf{k}), \quad (45)$$

where  $\zeta_{\alpha\beta, \mathbf{k}} = |\mathbf{R}_{\alpha\beta} + \mathbf{k}|/a$  and  $\mathbf{R}_{\alpha\alpha} = 0$ . Hence, except for  $v = n = 1$ , the RHS of (21) can be partitioned as the absolutely convergent sum (over  $\mathbf{k} \neq 0$ ) of near-field-like expressions, as if each particle were interacting with all others in the *infinite* system, except for the interactions included in  $\mathcal{A}^*$ . Following the way of reasoning of Section 2.6 we first introduce a new barrier function  $v^{**}(\alpha, \beta, n, \mathbf{k})$  (ensuring  $v^{**}(\alpha, \beta, 1, \mathbf{k}) > 0$ ) and restrict the summation over  $v$  by  $1 \leq v \leq v^{**}$ . Here  $v^{**}$  is the first value satisfying

$$Q_{v^{**}+1}(\zeta_\beta) \sum_{v=v^{**}+1}^{\infty} \frac{|\kappa| (v+n)!}{v! n! \zeta_{\alpha\beta, \mathbf{k}}^{v+n+1}} < \frac{\chi h N (\zeta_{\alpha\beta, \mathbf{k}})^{-4}}{\sum_{\alpha=1}^N \sum_{\beta=1}^N \sum_{\mathbf{k}}' (\zeta_{\alpha\beta, \mathbf{k}})^{-4}} \quad (46)$$

(if (46) is not met up to  $v^{**} = k_0 - 1$ , we set  $v^{**} = k_0$ ). The definition (46) and the inequality (40) rigorously imply that the norm (36) of the omitted terms in the partitioned expression (21) will also be less than  $\chi h$  if the estimate (35) is accepted. The definition (46) is based on the same principles as (42) for the near-field economization except that the upper summation bound and  $Q_v(\zeta_\beta)$  in the LHS are replaced by  $\infty$  and  $Q_{v^{**}+1}(\zeta_\beta)$ , respectively. These two modifications only increase the LHS, but very slightly if there are, at least, several particles in the cell  $V$ . At the same time, the form (46) enables fast computation of  $v^{**}$ , starting from the analytical expression for the LHS sum with  $v^{**} = 0$ . In the RHS of (46) the approximation used is

$$\sum_{\mathbf{k}}' (\zeta_{\alpha\beta, \mathbf{k}})^{-4} \approx \sum_{0 < k^2 \leq 5} (\zeta_{\alpha\beta, \mathbf{k}})^{-4} + a^4(5.31 + 0.64\mathbf{R}_{\alpha\beta}^2). \quad (47)$$

To restore the self-adjointness of  $\mathcal{A}^{**}$ , we proceed from  $v^{**}$  to two rougher bounds  $k_0^{**}(\alpha, \beta, \mathbf{k})$  and  $l^{**}(\alpha, \beta, \mathbf{k})$ . These functions obey

$$\begin{aligned} k_0^{**}(\beta, \alpha, \mathbf{k}) &= k_0^{**}(\alpha, \beta, -\mathbf{k}), \\ l^{**}(\beta, \alpha, \mathbf{k}) &= l^{**}(\alpha, \beta, -\mathbf{k}) \end{aligned} \quad (48)$$

and are defined for  $\zeta_\alpha \geq \zeta_\beta$  as

$$\begin{aligned} k_0^{**}(\alpha, \beta, \mathbf{k}) &= \max_{n: n \leq k_0, v^{**} > 0} \max(v^{**}, n), \\ l^{**}(\alpha, \beta, \mathbf{k}) &= \max_{n: n \leq k_0, v^{**} > 0} (n + v^{**}). \end{aligned} \quad (49)$$

Besides, we define the *symmetric* functions

$$\begin{aligned} k_0^{**}(\alpha, \beta) &= \max_{\mathbf{k} \neq 0} k_0^{**}(\alpha, \beta, \mathbf{k}) \\ l^{**}(\alpha, \beta) &= \max_{\mathbf{k} \neq 0} l^{**}(\alpha, \beta, \mathbf{k}). \end{aligned} \quad (50)$$

These two are also easy to calculate since they correspond to a minimum of  $|\mathbf{R}_{\alpha\beta} + \mathbf{k}|$ . For  $\mathbf{k} \rightarrow \infty$  we have  $l^{**}(\alpha, \beta, \mathbf{k}) \rightarrow \text{const}$  (equal to 2 or 3). It is essential that  $k_0^{**}(\alpha, \beta) \leq k_0$  and  $l^{**}(\alpha, \beta) \leq 2k_0$  for  $k_0, N \gg 1$ .

In the actual calculation the splitting of (21) into near-field-like terms is not performed. However, this imaginary partition allows us to construct the *economized* algorithm for  $\mathcal{A}^{**}$ :

1. Initialize  $(\mathcal{A}^{**}U)$ .
2. For all  $(\alpha, \beta)$ -pairs ( $1 \leq \alpha \leq \beta \leq N$ ):

2.1. For  $0 \leq m \leq n \leq k_0^{**}(\alpha, \beta)$  and  $v_0 = \min(k_0^{**}(\alpha, \beta), l^{**}(\alpha, \beta) - n)$  add the contribution

$$\frac{\kappa}{2} C_{nm} \sum_{v=1}^{v_0} (-1)^{v+m} C_{n+v, n-v} \sum_{\mu=-v}^v (S')_{\alpha\beta, v+n}^{\mu-m} C_{v\mu} U_{v\mu}^\beta \quad (51)$$

to  $(\mathcal{A}^{**}U)_{nm}^\alpha$  and simultaneously, if  $\alpha \neq \beta$ , the contribution

$$\frac{\kappa}{2} (-1)^{n+m} C_{nm} \sum_{v=1}^{v_0} C_{n+v, n-v} \sum_{\mu=-v}^v (S')_{\alpha\beta, v+n}^{\mu-m} C_{v\mu} U_{v\mu}^\alpha \quad (52)$$

to  $(\mathcal{A}^{**}U)_{nm}^\beta$ .

The lattice sums  $(S')_{\alpha\beta, v}^\mu$  for this algorithm are calculated "exactly" via Ewald transformation (Section 2.8) for  $v \leq N_E$  ( $N_E$  being a fixed parameter, usually 4 or 5) and by the direct summation (45) otherwise. It follows from the construction of  $l^{**}(\alpha, \beta, \mathbf{k})$  that, *still within the residual  $\chi h$* , the contribution of each term in the RHS of (45) to  $(S')_{\alpha\beta, v}^\mu$  can be restricted by  $N_E < v \leq l^{**}(\alpha, \beta, \mathbf{k})$ . To increase efficiency, a sufficient number of  $\mathbf{k}$ s are arranged in the order of ascending  $\mathbf{k}^2$  and the sum (45) is exhausted once  $l^{**}(\alpha, \beta, \mathbf{k}) \leq N_E$  for a whole layer  $\mathbf{k}^2 = \text{const}$ . The barriers  $k_0^{**}(\alpha, \beta)$ ,  $l^{**}(\alpha, \beta)$ , and, normally, all the necessary independent lattice sums are calculated before the iterations (the latter would be very prohibitive for the non-economical truncation (16) when  $k_0, N \gg 1$ ).

The efficiency of this algorithm for  $\mathcal{A}^{**}$  is characterized by

$$c_{ff} = \frac{1}{k_0^2(k_0+3)^2 N(N-1/2)} \times \left[ \sum_{1 \leq \alpha \leq \beta \leq N} \sum_{1 \leq n, v \leq k_0^{**}(\alpha, \beta), n+v \leq l^{**}(\alpha, \beta)} \mu_{\alpha\beta}(n+1)(v+1) \right] \quad (53)$$

(where  $\mu_{\alpha\alpha} = 2$ ,  $\mu_{\alpha\beta} = 8$  for  $\alpha \neq \beta$ ) which is, approximately, the number of FP multiplications (for the optimized code) relative to (17).

## 2.8. Fast Calculation of the Lower-Order Lattice Sums

Now, Ewald-like expressions for the sums  $(S')_{\alpha\beta, v}^\mu$  of arbitrary order are required. In addition to (45), for  $v=2$  the relations (13b), (19), and the periodicity of  $\mathcal{P}_{ij}$  [14] imply

$$(S')_{\alpha\beta, 2}^\mu = \frac{1}{C_{2,\mu}} \left( \frac{4\pi}{5} \right)^{1/2} \sum_{\mathbf{k}} \left[ \left( \frac{2}{\xi_{\alpha\beta, \mathbf{k}}} \right)^3 Y_{2,\mu}(\mathbf{R}_{\alpha\beta} + \mathbf{k}) - \left( \frac{2a}{|\mathbf{k}|} \right)^3 Y_{2,\mu}(\mathbf{k}) \right] \quad (54)$$

Using Maxwell relation for  $Y_{v\mu}$  [19] in the form  $(D_i = \partial/\partial x_i)$ ,

$$\frac{Y_{v\mu}(\mathbf{x})}{|\mathbf{x}|^{v+1}} = (-2)^v \left[ \frac{(2v+1)}{4\pi(2v)!} \right]^{1/2} C_{v\mu} (D_1 + i D_2)^\mu D_3^{v-\mu} \left( \frac{1}{|\mathbf{x}|} \right) \quad \text{for } \mu \geq 0, \quad (55)$$

as well as (A3)–(A5), (45), (54), one can obtain

$$(S')_{\alpha\beta, v}^\mu = \frac{(-4a)^{v+1}}{2[(2v)!]^{1/2}} \left\{ (D_1 + i D_2)^\mu D_3^{v-\mu} \times \left[ G(\mathbf{x}) + \frac{1}{|\mathbf{x}|} \right]_{|\mathbf{x}=\mathbf{R}_{\alpha\beta}} + \frac{4}{3} \pi \delta_{v,2} \delta_{\mu,0} \right\}. \quad (56)$$

Ewald representation for  $G(\mathbf{x})$  [20] yields

$$G(\mathbf{x}) + \frac{1}{|\mathbf{x}|} = - \sum_{\mathbf{k}} \frac{\exp(-\pi \mathbf{k}^2 - 2\pi i \mathbf{k} \cdot \mathbf{x})}{\pi \mathbf{k}^2} + \frac{2}{\pi^{1/2}} \int_0^{\pi^{1/2}} \exp(-\mathbf{x}^2 t^2) dt - \frac{2}{\pi^{1/2}} \sum_{\mathbf{k}} \int_{\pi^{1/2}}^{\infty} \exp[-(\mathbf{x}-\mathbf{k})^2 t^2] dt. \quad (57)$$

Using (57) and Rodrig formula for Hermite polynomials  $H_n(\xi)$  [17, 18], we arrive at

$$(-1)^{v+1} (D_1 + i D_2)^\mu D_3^{v-\mu} \left[ G(\mathbf{x}) + \frac{1}{|\mathbf{x}|} \right] = (2\pi i)^v \sum_{\mathbf{k}} \frac{(k_1 + i k_2)^\mu k_3^{v-\mu} \exp(-\pi \mathbf{k}^2 - 2\pi i \mathbf{k} \cdot \mathbf{x})}{\pi \mathbf{k}^2} - (x_1 + i x_2)^\mu I_v^\mu + \sum_{\mathbf{k}} (y_1 + i y_2)^\mu J_{v,\mathbf{k}}^\mu, \quad (58)$$

where

$$I_v^\mu = \frac{2^{\mu+1}}{\pi^{1/2}} \int_0^{\pi^{1/2}} t^{v+\mu} H_{v-\mu}(x_3 t) \exp(-\mathbf{x}^2 t^2) dt, \quad (59a)$$

$$J_{v,\mathbf{k}}^\mu = \frac{2^{\mu+1}}{\pi^{1/2}} \int_{\pi^{1/2}}^{\infty} t^{v+\mu} H_{v-\mu}(y_3 t) \exp(-\mathbf{y}^2 t^2) dt, \quad \mathbf{y} = \mathbf{x} - \mathbf{k}. \quad (59b)$$

The properties of  $H_n(\xi)$  [17, 18] yield the following, the most efficient computational scheme for  $J_{v,\mathbf{k}}^\mu$ :

$$J_{v+1,\mathbf{k}}^{v+1} = \frac{1}{y^2} [2(2\pi)^v \exp(-\pi \mathbf{y}^2) + (2v+1) J_{v,\mathbf{k}}^v], \quad (60a)$$

$$J_{v+1,\mathbf{k}}^\mu = y_3 J_{v+1,\mathbf{k}}^{\mu+1} - (v-\mu) J_{v,\mathbf{k}}^{\mu+1} \quad (\mu = v, v-1, \dots, 0), \quad (60b)$$

$$J_0^0 = \frac{1}{\pi \mathbf{y}^2} \exp(-\pi \mathbf{y}^2) \phi \left( \frac{1}{2\pi \mathbf{y}^2} \right). \quad (60c)$$

Instead of using ERFC and a square root, our algorithm calculates  $\phi(z)$  very efficiently (see Appendix C), taking only four multiplications and using a small amount (16 Kb) of additional memory. For  $I_v^\mu$  with  $\mathbf{x} \neq \mathbf{0}$  the Eqs. (60a)–(60b) also hold, with  $\mathbf{y} \leftarrow \mathbf{x}$  and the minus sign before the first term in the brackets (60a). Finally, for  $\mathbf{x} \rightarrow \mathbf{0}$  ( $\alpha = \beta$ ) the only essential elements of  $I_v^\mu$  are

$$I_{2n}^0 = 2(-\pi)^n (2n)!/[n!(2n+1)]. \quad (61)$$

In the algorithm the first sum (58) is truncated by  $\mathbf{k}^2 \leq R_E^2$ , the second one, by  $\mathbf{k}^2, (\mathbf{x} - \mathbf{k})^2 \leq R_E^2$ . The value  $R_E = 2.8$  was found to provide a great reserve of accuracy in the conductivity tensor for all applications. The optimized code reduces the calculation of all exponents in the sums (58) to simple multiplication of previously stored values. E.g.,  $\exp(-\pi \mathbf{y}^2)$  is written as  $((f_1(k_1) f_2(k_2)) f_3(k_3))$ , where

$$f_i(k_i) = \exp(-\pi x_i^2) \exp(-\pi k_i^2) [\exp(2\pi x_i)]^{k_i}, \quad (62)$$

with similar factorization of complex exponents (cf. with [21]).

### 2.9. Complementary Features of the Algorithm

The system (11) is iterated by the classical CGM in the form (see, e.g., [22]) which requires one computation of the LHS per iteration using three additional arrays, each as large as  $U_{nm}^z$ . The solution  $U_{nm}^z$  itself is easily eliminated (if the conductivity tensor is of only interest), providing a considerable memory saving. The initial vector  $\mathbf{U}_{(0)}$  is calculated from (11) in the “self-consistent” approximation (with zero  $S_{\alpha\beta, v+n}^{\mu-m}$ ). The process is terminated once the mean heat flux vector (14) stabilizes, to a given absolute accuracy, for three successive iterations (to ensure against a non-monotonic behavior). All the calculations are performed in double precision, and the results for  $\mathbf{F}$  in the tests always coincided, with a great reserve of accuracy, with those for the other, less efficient, self-correcting iterative schemes. The usual precision format is used only to store the lattice sums  $(S')_{\alpha\beta, v}^\mu$  (which proved acceptable, with a considerable reserve of accuracy). In case of insufficient memory to keep all the necessary elements  $(S')_{\alpha\beta, v}^\mu$  the rest of them are recalculated on the iterations.

It follows from Sections 2.6–2.7 that the norm of the residual in  $\mathcal{A}^* + \mathcal{A}^{**}$  due to economization is, at most,  $2\chi h$ . To compensate for the overestimation (which is likely to be considerable since the inequality  $\|\sum \dots\| \leq \sum \|\dots\|$  was used repeatedly) a relatively large value  $\chi = 5$  is chosen and shown to be reasonably good for all applications, at least, with  $N \geq 8$  (see Section 3).

Once  $\chi$  and  $N_E$  are fixed, we obtain a one-parameter family of modified  $k_0$ -approximations. Regardless of the considerations lying behind this construction the con-

vergence to the exact solution at  $k_0 \rightarrow \infty$  is ensured. It is clear intuitively since  $h \rightarrow 0$  and  $k_0^*, k_0^{**}, l^{**} \rightarrow \infty$  at  $k_0 \rightarrow \infty$ , so each element of  $\mathcal{A}^*$  ( $\mathcal{A}^{**}$ ) is eventually included and the accuracy of lattice sum calculation grows infinitely. (The convergence of  $\mathcal{A}^* + \mathcal{A}^{**}$  to the triple sum operator (11) in the norm induced by (36) can be proved rigorously for non-touching spheres.) On the other hand, the method is flexible since for fixed  $k_0$  and  $\chi \rightarrow 0$  the limit of the non-economical solution (i.e., the truncation (16) alone with the exact lattice sums) is achieved.

For  $N \geq 1$  some insignificant simplifications of the algorithm for  $\mathcal{A}^{**}$  could be made, but the present version was constructed to work well both for large and for small  $N > 1$ . The length of the optimized code is about 1500 Fortran-77 lines. The memory requirement for  $k_0, N \geq 1$  is approximately

$$24(k_0 + 1)(k_0 + 2)(N + 1) + 3N(N + 33) + 8k_0(N + 2k_0 + 16) + 20,000 \quad (63)$$

bytes, without the space for  $(S')_{\alpha\beta, v}^\mu$ .

### 3. NUMERICAL RESULTS AND THE EFFICIENCY OF THE ALGORITHM

For test purposes, the calculations were performed with 27 superconducting spheres located regularly in the cell so that the periodically replicated system is a simple cubic array. For  $c = 0.522$ ,  $\chi = 5$ ,  $N_E = 5$  the effective relative conductivity was found to be 9.93 ( $k_0 = 40$ ), 10.123 ( $k_0 = 50$ ), and 10.133 ( $k_0 = 63$ ), with the excellent convergence to the result [23] 10.14. For  $k_0 = 50$  the value 10.12 was attained after 10 iterations ( $\approx 30$  min)<sup>1</sup>.

As the second, and decisive, test for our code, the comparison was made with the direct numerical solution of the BIE system (5) for the random configuration with  $c = 0.5$ ,  $N = 8$ ,  $\gamma = 20$ , obtained by the Metropolis method [24] for “hard spheres” (for details, see Appendix D). Table I shows that in our case the convergence of BIEM is rather slow as the number  $N_T$  of triangle elements per sphere tends to infinity, if no special measures (e.g., the improvement [25]) are undertaken. However, the linear (in  $N_T^{-1}$ ) extrapolation of  $F_{11}, F_{21}, F_{31}$  for  $N_T = 320, 1280$  yields the values 3.78, 0.025, 0.108, close to those for our method at  $k_0 \rightarrow \infty$ . The CPU time per iteration was about 6 h for BIEM at  $N_T = 1280$ , compared to 7.5 (14) s for our code at  $k_0 = 20$  (25). It should be noted, however, that BIEM is a universal algorithm for arbitrary-shaped inclusions and, not surprisingly, turns out to be much slower than the present highly specialized algorithm for spheres.

<sup>1</sup> This is much faster than about 30 min on a CRAY Y-MP to obtain similar accuracy for  $c \leq 0.520$  by the random walker method [3].

TABLE I

Comparison of the Present Method with the Boundary Integral Equation Method for the Random Configuration with  $c=0.5$ ,  $N=8$ ,  $\gamma=20$

BIEM				The present method, $\chi=5$ , $N_E=6$						
$N_T$	20	80	320	1280	$k_0$	5	10	15	20	25
$F_{11}$	1.844	2.824	3.442	3.693	$F_{11}$	3.699	3.787	3.799	3.802	3.803
$F_{21}$	0.000	0.002	0.012	0.022	$F_{21}$	0.014	0.025	0.027	0.028	0.028
$F_{31}$	0.003	0.036	0.073	0.099	$F_{31}$	0.084	0.106	0.109	0.110	0.110

Note. The list of particle coordinates (as well as for the other configurations studied in the present paper) is available on the request from the author.

In the latter case the effect of economization is less pronounced (i.e., for  $k_0=20$  the acceleration factor  $(c_{nf} + c_{ff})^{-1}$  is "only" 5.2) so it is of interest to test our method for larger random systems. Table II presents, for several configurations, the values of  $F_{11}$  for the economical solution ( $\chi=5$ ), along with the corresponding inverse efficiency coefficients  $c_{nf}$ ,  $c_{ff}$ , the actual CPU times  $T_0$  (s) for the pre-iterative part and  $T_{ii}$  (s) per iteration, as well as the amount  $M_S$  (Kb) of the computer memory sufficient to

TABLE II

On the Efficiency of the Algorithm (for Details, see the Text)

	$k_0$	$F_{11}$	$F'_{11}$	$c_{nf}$	$c_{ff}$	$T_0$	$T_{ii}$	$M_S$
1. Equilibrium state, $c=0.45$ , $\gamma=\infty$ , $N=125$ , $N_E=4$	5	4.165	4.188	$9.0 \times 10^{-2}$	$1.1 \times 10^{-2}$	161	17	163
	10	4.342	4.354	$2.2 \times 10^{-2}$	$3.8 \times 10^{-3}$	222	35	372
	15	4.375	4.403	$9.0 \times 10^{-3}$	$8.8 \times 10^{-4}$	224	50	372
	20	4.411	4.423	$5.1 \times 10^{-3}$	$3.8 \times 10^{-4}$	238	70	419
	25	4.426	4.432	$3.3 \times 10^{-3}$	$3.1 \times 10^{-4}$	289	100	615
	30*	4.437	4.438	$2.3 \times 10^{-3}$	$1.7 \times 10^{-4}$	47	384	651
2. Metastable state, $c=0.59$ , $\gamma=100$ , $N=125$ , $N_E=4$	5	6.352	6.312	$1.2 \times 10^{-1}$	$4.0 \times 10^{-2}$	218	24	372
	10	6.821	6.822	$3.2 \times 10^{-2}$	$3.8 \times 10^{-3}$	220	45	372
	15	6.965	6.952	$1.5 \times 10^{-2}$	$1.1 \times 10^{-3}$	235	73	413
	20	6.994	6.998	$9.6 \times 10^{-3}$	$7.5 \times 10^{-4}$	296	120	637
	25	7.014	7.017	$6.9 \times 10^{-3}$	$3.3 \times 10^{-4}$	299	178	651
	30*	7.027	7.026	$5.2 \times 10^{-3}$	$1.7 \times 10^{-4}$	49	505	663
3. Metastable state, $c=0.59$ , $\gamma=30$ , $N=125$ , $N_E=4$	5	5.278	5.263	$1.4 \times 10^{-1}$	$4.0 \times 10^{-2}$	221	26	372
	10	5.521	5.514	$3.4 \times 10^{-2}$	$4.0 \times 10^{-3}$	225	47	383
	15	5.560	5.561	$1.7 \times 10^{-2}$	$2.2 \times 10^{-3}$	296	84	644
	20	5.574	5.574	$1.1 \times 10^{-2}$	$7.8 \times 10^{-4}$	301	131	652
4. Equilibrium state, $c=0.6$ , $\gamma=\infty$ , $N=64$ , $N_E=4$	5	6.361	6.313	$1.7 \times 10^{-1}$	$4.0 \times 10^{-2}$	57	8	97
	10	6.597	6.589	$4.9 \times 10^{-2}$	$5.2 \times 10^{-3}$	62	16	114
	15	6.659	6.648	$2.5 \times 10^{-2}$	$2.3 \times 10^{-3}$	77	30	170
	20	6.676	6.671	$1.5 \times 10^{-2}$	$8.4 \times 10^{-4}$	78	47	176
	30	6.685	6.689	$7.5 \times 10^{-3}$	$2.9 \times 10^{-4}$	81	94	227
	40	6.696	6.695	$4.4 \times 10^{-3}$	$1.2 \times 10^{-4}$	85	157	267
5. Metastable state, $c=0.585$ , $\gamma=0$ , $N=27$ , $N_E=5$	5	0.2894	0.2894	$3.3 \times 10^{-1}$	$2.2 \times 10^{-1}$	17	3	46
	10	0.2861	0.2861	$1.1 \times 10^{-1}$	$3.4 \times 10^{-2}$	18	7	60
	15	0.2856	0.2856	$5.8 \times 10^{-2}$	$1.0 \times 10^{-2}$	18	13	70
	20	0.2855	0.2855	$3.9 \times 10^{-2}$	$4.4 \times 10^{-3}$	18	21	79

keep all the necessary lattice sums.<sup>2</sup> Besides,  $F'_{11}$  denotes the values of  $F_{11}$  for the hypothetical non-economical solution (11), (16) (to obtain these, it was sufficient to set  $\chi=0.5$ , 0.05 in the limit process  $\chi \rightarrow 0$  for fixed  $k_0$ ). Each run took 12–21 iterations, with the error in tabulated  $F_{11}$ ,  $F'_{11}$  not exceeding a unit in the last decimal place. The metastable states were generated by the fast polydisperse densification method [10] with different kinetics. For  $N \gg 1$  and particle volume fraction  $c$  above the liquid–solid phase transition region,  $0.49 < c < 0.55$ , the configurations prepared by a densification procedure are metastable to Metropolis' stochastic mixing, with a very long computational life-time (the problem of phase transition is discussed, e.g., in [6]). In example 4, however, the metastability was destroyed after a few million of additional Metropolis' scheme steps and the true equilibrium state of a "crystalline solid" was achieved. For this example the advantage of CGM over the simple iteration method was tested (i.e., to obtain a 1% accuracy of  $F_{11}$ , the two methods required six and 26 iterations, respectively). In case 1 the results for conductivity are untypically high since for the other equilibrium states with the same  $c$ ,  $N$ ,  $\gamma$  the exact values of  $F_{ii}$  ( $F'_{ii}$ ) are usually about 4.1.

Table II clearly demonstrates that the values of  $F_{11}$  are practically no worse than  $F'_{11}$ , but that the former are obtained much faster than by the non-economical solution (e.g., for case 2 with  $k_0=20$  the acceleration factor  $(c_{nf} + c_{ff})^{-1}$  equals 97). The values of  $F_{11}$  are sometimes even closer to the exact solution obviously because the near- and far-field economizations may act in opposite directions. If necessary, these oscillations can be strongly suppressed by choosing a smaller value  $\chi \approx 1$  for the far-field economization, with a slight decrease in  $(c_{nf} + c_{ff})^{-1}$ . The method retains the efficiency for touching spheres of finite conductivity, when only the weak convergence of  $\mathcal{A}^* + \mathcal{A}^{**}$  at  $k_0 \rightarrow \infty$  can be shown analytically.

It is of interest to check a posteriori the estimate (35) for a system with periodic replication. It is seen from Fig. 4 (cf. Figs. 1–3) that the ratios  $U_n^z/Q_n(\zeta_d)$  remain narrow-bounded for all  $n \geq 1$ , although being far from unity for high  $c$ . If a constant, concentration-dependent factor were introduced in (35), this would not affect the basic relations (42) and (46). That is the reason for the efficiency of the present method in the wide range of concentrations.

The very different method of estimating the effective conductivity of a disordered composite medium has been recently developed [2–3] based on random walking with different speeds in each phase. This approach is attractive because of its relative simplicity, particularly, for large arrays of non-spherical inclusions when the use of other

<sup>2</sup> In the runs of Table II marked by an asterisk almost all the lattice sums were recomputed on the iterations. However, less than  $M_S$  Kb of additional core would suffice to reduce  $T_{ii}$  from 384 s and 505 s to about 130 s and 250 s, respectively.

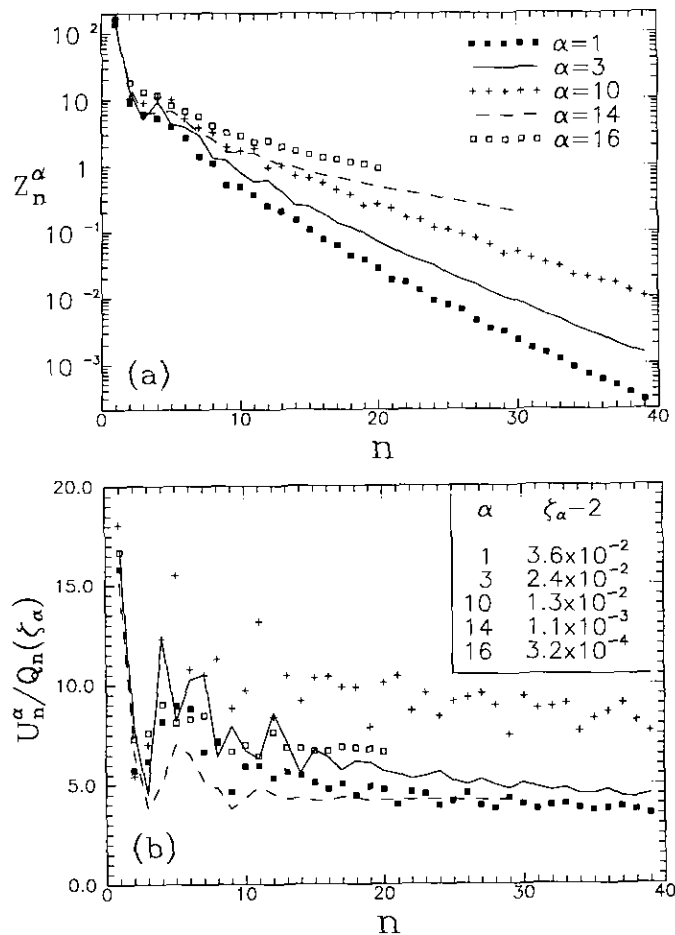


FIG. 4. The convergence-tested results ( $k_0 = 50, 72$ ) for the Fourier coefficients for the random configuration of 16 particles with periodic continuation:  $c = 0.55$ ,  $\gamma = 50$ ,  $\mathbf{K} = (0, 0, 1)$  ( $F_{33}^{\text{exact}} = 8.74$ ).

methods may be hampered. However, to obtain meaningful results even for spheres, the method may require a considerable amount of a supercomputer run time. It follows from [3] that for  $N = 125$  and  $0.1 \leq c \leq 0.6$  each configuration takes, *on the average*, about 120 s for  $\gamma = \infty$  and 240 s for  $\gamma = 10$  on a CRAY Y-MP, the accuracy in the effective conductivity being within 2%. (The run times for the extreme case  $c = 0.6$  were not reported.) In the interesting case,  $1 \ll \gamma < \infty$ , this direct method should become more expensive since a random walker is trapped inside the inclusions, with the small probability  $p_1 \approx 1/(\gamma + 1)$  of jumping into the continuous phase from the interface [2–3]. Judging by, *at least*, two-fold time saving for  $\gamma = \infty$  (when the special modification [2–3] eliminates random walking inside the spheres), one can estimate that, within the same accuracy, the run time for  $\gamma = 100$  would be, at least, 5.5 times larger than for  $\gamma = 10$ , thus exceeding 1300 s.

Our method appears to be comparatively fast, at least, for  $N$  up to hundreds. Even if (11) is solved three times to obtain the isotropic constituent  $\frac{1}{3}F_i^i \mathbf{I}$  of the conductivity

tensor (the pre-iterative part being performed only once) and a coarse accuracy of 2% accepted, then a “typical” metastable configuration with  $c = 0.59$ ,  $N = 125$  takes about 2220, 1000, 1550 s for  $\gamma = \infty^3$  (five iterations,  $k_0 = 20$ ),  $\gamma = 10$  (three iterations,  $k_0 = 10$ ), and  $\gamma = 100$  (five iterations,  $k_0 = 15$ ), respectively, on a PC AT ACRO 386 C/Weitek 3167 (a machine with  $2.5L \mu\text{s}$  execution time for a scalar product of two double precision vectors of the length  $L$ ). Note that the inner loops of our codes for  $\mathcal{A}^*$  ( $\mathcal{A}^{**}$ ) are all vectorizable. Moreover, the calculations for different  $(\alpha, \beta)$ -pairs therein are ideal for parallelization on a supercomputer since they can be made almost non-conflicting in memory access using about  $67k_0^2$  additional doublewords (for 8 CPUs). Taking also into account the rate of chained operations on a CRAY X-MP [26, Table 7] and a faster clock period (6 ns) of Y-MP one can realistically estimate that, even with the vector length degradation for small  $k_0$ , the reported run times for our algorithm would undergo from 65-fold (for a single CPU used) to about 500-fold decrease (for 8 CPUs) on a CRAY Y-MP. Despite uncertainties in the reported run times for the algorithm [3] this comparison shows a many-fold advantage for the present method. Besides, high accuracy can be easily achieved in our algorithm. For the other concentrations, if the averaging over many configurations is required, the program parameters can be also adjusted to the whole set, as for two-dimensional simulations [10].

For very large  $N \geq 10^3$  a possible improvement of our algorithm would be to calculate  $(S')_{\alpha\beta, \nu}^{\nu}$  via the symmetry relations and interpolation using the tabulated values of (58) in the range  $0 \leq x_1 \leq x_2 \leq \frac{1}{2}$ ,  $x_3 \leq \frac{1}{2}$ . However, too large values of  $N$  can be often avoided in the applications due to periodic continuation.

#### 4. CONCLUSIONS

The algorithm has been constructed for the efficient solution of  $N$ -particle heat interaction problem in a concentrated random dispersion of spheres with the periodic continuation. The method is capable to provide high resolution for arbitrary conductivity ratio  $\gamma = \lambda/\lambda_e$  and has a moderate execution time for  $N$  up to hundreds even on a small computer. Our algorithm takes full advantage of the particle shape and is shown to operate much faster than the more general boundary element and random walking simulation methods. The generalization for arbitrary periods of continuation is straightforward. The rotational part of the algorithm is also the fast method for a finite cloud of particles, without periodic continuation.

By averaging over configurations, the present method enables high accuracy calculating the effective conductivity

<sup>3</sup> In particular, for the configuration 2–3 of Table II with  $\gamma = \infty$  we have  $F_{11} = 7.98$  (8.03) for  $k_0 = 20$  (30).

of dispersions with arbitrary microstructures. Besides, the attractive application of our algorithm is to study systematically the conduction through a *random close packing* of spheres with large but finite  $\gamma$ . For this case the theory [11] (which includes some empirical information) is well known, but successful simulations are still lacking.

The principles of economical solution of multiparticle problems developed in the present paper are expected to be even more essential for elastic interaction of (nearly) stiff inclusions in random composites and for hydrodynamic interaction of spheres in concentrated suspensions, when the singularity in the regions of small gaps is stronger (cf. [11, 27–28]) and it is of vital importance to retain higher-order harmonics.

#### APPENDIX A: DERIVATION OF (11)

The integrals ( $d\Omega = dS/a^2$ )

$$\int_{S_\alpha} \bar{Y}_{nm}(\mathbf{x} - \mathbf{x}^\alpha) d\Omega_{\mathbf{x}} \left[ \int_{S_\beta} \frac{\partial G(\mathbf{y} - \mathbf{x})}{\partial n_y} Y_{\nu\mu}(\mathbf{y} - \mathbf{x}^\beta) d\Omega_y \right], \quad (\text{A1})$$

occurring after substituting (8) into (5), can be evaluated as follows:

1.  $\alpha \neq \beta$ . The function  $G(\mathbf{y} - \mathbf{x})$  in (A1) can be replaced by

$$\tilde{G}(\mathbf{x}, \mathbf{y}) = G(\mathbf{y} - \mathbf{x}) + \frac{2}{3}\pi |\mathbf{y} - \mathbf{x}^\beta|^2 + \frac{2}{3}\pi |\mathbf{x} - \mathbf{x}^\alpha|^2 \quad (\text{A2})$$

which is a harmonic function of  $\mathbf{x}$  and  $\mathbf{y}$ . Expanding  $\tilde{G}$  into Taylor double series at  $\mathbf{y} = \mathbf{x}^\beta$  and  $\mathbf{x} = \mathbf{x}^\alpha$ , using the connection between harmonic polynomials and spherical harmonics [17, 19], as well as the orthogonality of  $Y_{\nu\mu}$  ( $Y_{nm}$ ) on  $S_\beta$  ( $S_\alpha$ ) one can prove that for  $\nu, n \geq 1$  the integral (A1) is a certain linear combination of the derivatives  $\partial^{n+\nu} G(\mathbf{x}) / \partial x_1^p \partial x_2^q \partial x_3^r$  at  $\mathbf{x} = \mathbf{x}^\beta - \mathbf{x}^\alpha$ . For  $n = \nu = 1$  the relation [14] used is

$$\frac{\partial^2 G(\mathbf{x})}{\partial x_i \partial x_j} = -\mathcal{P}_{ij}(\mathbf{x}) - \frac{4}{3}\pi \delta_{ij}, \quad (\text{A3})$$

where  $\delta_{ij}$  is the Kronecker delta and  $\mathcal{P}_{ij}(\mathbf{x})$  is the three-dimensional analogue of the Weierstrass function

$$\mathcal{P}_{ij}(\mathbf{x}) = \frac{\partial^2 (|\mathbf{x}|^{-1})}{\partial x_i \partial x_j} + \sum_{\mathbf{k}} \left[ \frac{\partial^2 (|\mathbf{x} + \mathbf{k}|^{-1})}{\partial x_i \partial x_j} - \frac{\partial^2 (|\mathbf{x}|^{-1})}{\partial x_i \partial x_j} \Big|_{\mathbf{x}=\mathbf{k}} \right] \quad (\text{A4})$$

with the prime denoting the exclusion of  $\mathbf{k} = 0$  from the summation, as usual. It follows from (A3) that for  $\nu = n = 1$  the integral (A1) takes the form  $(\frac{2}{3}\pi)^2 a \delta_{m\mu}$  plus the addi-

tional term arising from  $-\mathcal{P}_{ij}$  in the RHS of (A3). Besides, the identity [14]

$$\frac{\partial^{p+q+r} G(\mathbf{x})}{\partial x_1^p \partial x_2^q \partial x_3^r} = - \sum_{\mathbf{k}} \frac{\partial^{p+q+r} (|\mathbf{x} + \mathbf{k}|^{-1})}{\partial x_1^p \partial x_2^q \partial x_3^r} \quad (\text{for } p+q+r > 2) \quad (\text{A5})$$

and the above reasoning rigorously imply that for  $n + \nu > 2$  the integral (A1) can be evaluated as if  $G(\mathbf{y} - \mathbf{x})$  were represented by the formal sum  $-\sum |\mathbf{y} - \mathbf{x} + \mathbf{k}|^{-1}$ . In both cases, to complete the calculation, the only expression for (A1) with  $G(\mathbf{y} - \mathbf{x}) = -|\mathbf{y} - \mathbf{x}|^{-1}$  is required. The latter can be obtained using the relation [19]

$$\int_{S_\beta} \frac{\partial |\mathbf{x} - \mathbf{y}|^{-1}}{\partial n_y} Y_{\nu\mu}(\mathbf{y} - \mathbf{x}^\beta) d\Omega_y = \frac{4\pi\nu a^{\nu-1} Y_{\nu\mu}(\mathbf{x} - \mathbf{x}^\beta)}{(2\nu + 1) |\mathbf{x} - \mathbf{x}^\beta|^{\nu+1}} \quad (\text{for } |\mathbf{x} - \mathbf{x}^\beta| > a), \quad (\text{A6})$$

the generalized addition theorem [12, 29]

$$\begin{aligned} & \frac{Y_{\nu\mu}(\mathbf{x} - \mathbf{x}^\beta)}{|\mathbf{x} - \mathbf{x}^\beta|^{\nu+1}} \\ &= \left[ \frac{2\nu + 1}{(\nu - \mu)! (\nu + \mu)!} \right]^{1/2} \sum_{n=0}^{\infty} \sum_{m=-n}^n (-1)^{\nu+m} \\ & \times \left[ \frac{4\pi(\nu + n + \mu - m)! (\nu + n + m - \mu)!}{(2n + 1)(2\nu + 2n + 1)(n - m)! (n + m)!} \right]^{1/2} \\ & \times \frac{Y_{\nu+n, \mu-m}(\mathbf{x}^\beta - \mathbf{x}^\alpha)}{|\mathbf{x}^\beta - \mathbf{x}^\alpha|^{\nu+n+1}} |\mathbf{x} - \mathbf{x}^\alpha|^n Y_{nm}(\mathbf{x} - \mathbf{x}^\alpha) \quad (\text{A7}) \end{aligned}$$

and the orthogonality of  $Y_{nm}$  on  $S_\alpha$ .

2.  $\alpha = \beta$ . In this case we have  $G(\mathbf{y} - \mathbf{x}) = -|\mathbf{y} - \mathbf{x}|^{-1} + g(\mathbf{y} - \mathbf{x})$ , where  $g$  is a regular function of  $\mathbf{x}, \mathbf{y}$  inside  $S_\alpha$ . The contribution of the first term to (A1) can be found using the relation

$$\begin{aligned} & \int_{S_\alpha} \frac{\partial |\mathbf{x} - \mathbf{y}|^{-1}}{\partial n_y} Y_{\nu\mu}(\mathbf{y} - \mathbf{x}^\alpha) d\Omega_y \\ &= -\frac{2\pi Y_{\nu\mu}(\mathbf{x} - \mathbf{x}^\alpha)}{a^2(2\nu + 1)} \quad (\text{for } \mathbf{x} \in S_\alpha) \quad (\text{A8}) \end{aligned}$$

(which follows from (A6) at  $\mathbf{x} \rightarrow S_\beta$ ) and the orthogonality of  $Y_{nm}$ . The contribution of  $g(\mathbf{y} - \mathbf{x})$  to (A1) is again a linear combination of  $\partial^{n+\nu} g(\mathbf{x}) / \partial x_1^p \partial x_2^q \partial x_3^r$  at  $\mathbf{x} = 0$  and can be evaluated in the same manner as for  $\alpha \neq \beta$ . Namely, (A3) and (A5) are applied to  $g(\mathbf{x})$  at  $\mathbf{x} = 0$ , with  $\mathcal{P}_{ij} = 0$  and  $\sum$  replaced by  $\sum'$ .

Summing up the above arguments yields the explicit form (11) of the system for the unknowns  $U_{nm}^\alpha$ .

## APPENDIX B: ANALYTICAL RESULTS FOR FOURIER COEFFICIENT DECREASE

For  $\zeta \neq 2$  the asymptotics  $U_{nm} \simeq q^n A(n)$  is assumed, with the unknown  $q \in (0, 1)$  and some "slowly varying" function  $A(n)$ . From the Stirling formula we have for  $n, v \gg 1$  at  $v = v_0$

$$\frac{(n+v)! \zeta^{-(n+v+1)} q^v}{[(n-m)!(n+m)!(v-m)!(v+m)!]^{1/2}} \simeq \frac{\exp[-(v-v_0)^2(\zeta-q)^2/(2\zeta nq)]}{(2\pi\zeta nq)^{1/2}(\zeta-q)^n},$$

$$v_0 = \frac{nq}{\zeta - q}. \quad (\text{B1})$$

The expression (B1), as a function of  $v$ , is sharply peaked at  $v = v_0$ . Hence, on substituting  $U_{nm}$  and (B1) into (34)  $A(v)$  (treated as a continuous function) can be replaced by  $A(v_0)$ . Proceeding from summation to integration near  $v = v_0$  yields a quadratic equation for  $q$  and a functional one for  $A(n)$ , resulting in

$$U_{nm} \sim q^n n^{-\delta}, \quad q = \frac{\zeta - (\zeta^2 - 4)^{1/2}}{2},$$

$$\delta = \frac{\ln(\kappa_m q)}{2 \ln q} \quad (\text{for } \zeta > 2, \kappa \in [-1, 1]). \quad (\text{B2})$$

For  $\kappa_m < 0$   $n^{-\delta}$  is replaced by a linear combination of its real and imaginary parts.

For touching spheres the asymptotics of  $U_{nm}$  is sought in the form  $n^{-\delta} \exp(-\beta n^{1/2})$  using (B1) with  $q = 1$  and  $\zeta = 2$ . Approximating  $v^{1/2}$  by a linear function at  $v = v_0 = n$ , replacing  $v^{-\delta}$  by a constant  $n^{-\delta}$ , and proceeding to integration, we arrive at the equation for  $\beta$ . However, this simple method gives no result for  $\delta$ , and the analytical study is complemented by the numerical solution of (34) to yield the contact asymptotics:

$$U_{nm} \sim n^{-\delta} \exp\{-2[n \ln(\kappa_m^{-1})]^{1/2}\}, \quad (\text{B3a})$$

$$\delta = \begin{cases} \frac{1}{4} & (\text{for } \kappa_m \neq 1) \\ \frac{1}{2} & (\text{for } \kappa = 1, m = 0) \\ \frac{3}{2} & (\text{for } \kappa = -1, m = 1). \end{cases} \quad (\text{B3b})$$

Again, for  $\kappa_m < 0$  a linear combination of real and imaginary parts of the RHS in (B3a) is taken.

## APPENDIX C: FAST COMPUTATION OF $\phi(z)$

First, the values of  $h^k \phi^{(k)}(z)/k!$  ( $h = 2/(\pi M)$ ) for  $k \leq 3$  are tabulated to machine double precision on a uniform mesh  $0 = z_0 < z_1 < \dots < z_M = 2/\pi$  (the segment  $[0, 2/\pi]$  includes all the necessary arguments of  $\phi(z)$  for the problem at

hand). The higher derivatives can be expressed via  $\phi(z)$  by differentiating the relation

$$\phi'(z) = [1 - (1+z)\phi(z)]/(2z^2) \quad (\text{C1})$$

but this way is not good for small  $z$  because of the rapid loss of accuracy. Instead, starting from the continued fraction representation [30]

$$\phi(z) = 1/(1 + z/(1 + 2z/(1 + 3z/\dots))) \quad (\text{C2})$$

and (C1), one can derive the computationally stable relations

$$\phi^{(k)}(z) = \frac{(-1)^k k! (2k-1)!! D_{2k}}{\prod_{j=1}^{2k} (1 + jz D_j)} \quad \text{for } k \geq 0,$$

$$D_j = 1/[1 + (j+1)z/[1 + (j+2)z/\dots]] \quad (\text{C3})$$

$$= 1/[1 + (j+1)z D_{j+1}].$$

Once  $h^k \phi^{(k)}/k!$  have been tabulated,  $\phi(z)$  is computed as a four-term Taylor expansion at the nearest mesh point. For  $M = 500$  the maximum and average relative error in  $\phi(z)$  is  $10^{-10}$  and  $\approx 10^{-12}$ , respectively.

## APPENDIX D: DETAILS OF BIEM TEST

The convenient way [4] was used to approximate each sphere by a set of planar triangle elements  $\Delta_i^\alpha$  ( $i = 1, \dots, N_T$ ) with centroids  $\mathbf{O}_i^\alpha$  and  $T^*$  taken as a constant over  $\Delta_i^\alpha$ . To approximate the integral over  $\Delta_j^\beta$ , this element is shifted periodically to minimize  $|\mathbf{O}_j^\beta - \mathbf{O}_i^\alpha|$ , then  $G(\mathbf{y} - \mathbf{O}_i^\alpha) = -|\mathbf{y} - \mathbf{O}_i^\alpha|^{-1} + G_1$  within  $\Delta_j^\beta$ . The regular part  $\partial G_1/\partial n_y$  is taken as a constant, so is  $\partial |\mathbf{y} - \mathbf{O}_i^\alpha|^{-1}/\partial n_y$  for  $|\mathbf{O}_j^\beta - \mathbf{O}_i^\alpha|^2 > \rho \Delta S_j$  ( $\rho \geq 30$ ,  $\Delta S_j$  is the element area). For nearby elements (with  $\Delta_j^\beta \neq \Delta_i^\alpha$ ) the singular part is integrated exactly by the spherical trigonometry formulae [18]. The values of  $\nabla G_1$  are obtained by the symmetry relations and linear interpolation from the table of Ewald-calculated vectors  $\nabla G_1(\mathbf{x})$  in the cube  $0 \leq x_k \leq \frac{1}{2}$ . Both  $30 \times 30 \times 30$  and  $49 \times 49 \times 49$  grids were used, with negligible change in the results for  $F_{ij}$ . The Seidel method was applied and  $\rho$  increased on the last iterations to approach the limit  $\rho = \infty$ .

## ACKNOWLEDGMENT

The author thanks Professor S. Kim (University of Wisconsin) for making available his works on the boundary integral equation method in multiparticle problems.

## REFERENCES

1. A. S. Sangani and C. Yao, *J. Appl. Phys.* **63**, 1334 (1988).
2. I. C. Kim and S. Torquato, *J. Appl. Phys.* **68**, 3892 (1990).
3. I. C. Kim and S. Torquato, *J. Appl. Phys.* **69**, 2280 (1991).

4. S. Kim and S. J. Karrila, *Microhydrodynamics: Principles and Selected Applications* (Butterworth-Heinemann, Boston, 1991).
5. R. T. Bonnecaze and J. F. Brady, *Proc. R. Soc. London A* **430**, 285 (1990).
6. R. T. Bonnecaze and J. F. Brady, *Proc. R. Soc. London A* **432**, 445 (1991).
7. A. S. Sangani and C. Yao, *Phys. Fluids* **31**, 2426 (1988).
8. P. P. Durand and L. H. Ungar, *Int. J. Numer. Methods Eng.* **26**, 2487 (1988).
9. A. Z. Zinchenko, *Zh. Tekh. Fiz.* **59**(1), 29 (1989) [Russian]; Engl. transl., *Sov. Phys. Tech. Phys.* **34**, 15 (1989).
10. A. Z. Zinchenko, *Zh. Tekh. Fiz.* **60**(11), 11 (1990) [Russian]; Engl. transl., *Sov. Phys. Tech. Phys.* **35**, 1236 (1990).
11. G. K. Batchelor and R. W. O'Brien, *Proc. R. Soc. London A* **355**, 313 (1977).
12. K. Gunter and D. Heinrich, *Z. Phys.* **185**, 345 (1965).
13. L. C. Biedenharn and J. D. Louck, *Angular Momentum in Quantum Physics: Theory and Application* (Addison-Wesley, Reading, MA, 1981).
14. V. L. Berdichevsky, *Variational Principles of Continuum Mechanics* (Nauka, Moscow, 1983). [Russian]
15. H. Hasimoto, *J. Fluid Mech.* **5**, 317 (1959).
16. D. J. Jeffrey, *Proc. R. Soc. London A* **335**, 355 (1973).
17. A. F. Nikiforov and V. B. Uvarov, *The Foundations of Special Function Theory* (Nauka, Moscow, 1974). [Russian]
18. G. A. Korn and T. M. Korn, *Mathematical Handbook for Scientists and Engineers* (McGraw-Hill, New York, 1968).
19. E. W. Hobson, *The Theory of Spherical and Ellipsoidal Harmonics* (Chelsea, New York, 1955).
20. D. J. Adams and G. S. Dubey, *J. Comput. Phys.* **72**, 156 (1987).
21. M. J. L. Sangster and M. Dixon, *Adv. Phys.* **25**, 247 (1976).
22. R. W. Hockney and J. W. Eastwood, *Computer Simulation Using Particles* (McGraw-Hill, New York, 1981).
23. R. C. McPhedran and D. R. McKenzie, *Proc. R. Soc. London A* **359**, 45 (1978).
24. N. A. Metropolis, A. W. Rosenbluth, M. N. Rosenbluth, A. N. Teller, and E. Teller, *J. Chem. Phys.* **21**, 1087 (1953).
25. T. A. Cruse, *Comput. Struct.* **4**, 741 (1974).
26. M. L. Simmons and H. J. Wasserman, *J. Supercomput.* **4**, 153 (1990).
27. R. M. Christensen, *Mechanics of Composite Materials* (Wiley-Interscience, New York, 1979).
28. D. A. Cooley and M. E. O'Neill, *Mathematika* **16**, 37 (1969).
29. D. R. McKenzie, R. C. McPhedran, and G. H. Derrick, *Proc. R. Soc. London A* **362**, 211 (1978).
30. M. Abramowitz and I. A. Stegun (Eds.), *Handbook of Mathematical Functions*, NBS Appl. Math. Ser., Vol. 55, (Flammarion, Paris, 1964).